بِسْمِ ٱللَّهِ ٱلرَّحْمَٰنِ ٱلرَّحِيمِ

الجامعة اللبنانية
كلية الهندسة

Anadolu-Sham COMSAT
Communication Platforms & Satellite Communication Systems

Project N° :
88/2497
89/2498
2023 / 2024

FINAL YEAR PROJECT

Submitted in fulfillment of the requirements for the

ENGINEERING DEGREE FROM THE LEBANESE UNIVERSITY
BRANCH 1

Major : Mechanical Engineering in Energy

Done by

Jana Hammoud & Roukaya Al Samad

Design of a LOX/LCH4 Thruster Engine with a Pressure Feed System for Satellite Transfer from LEO to GEO, with Regenerative Cooling and Heat Recovery using RPA

Supervisor:
Dr. Fadi Taychouri

Defended on December --, 2024 in front of the jury:

Dr. Fadi Taychouri	President
Dr. Mohammad Abdel-Wahab	Member
Eng. Loubna Khaled	Member

Acknowledgments

All praise is due to Allah, by whose grace righteous deeds are completed. Through His mercy and blessings, we have achieved this milestone, which we take great pride in today. We ask Allah to accept our efforts and guide us toward what is best for us in this life and the hereafter. It is through His divine will that we have been able to persevere on this path despite the challenges. We hope this work will be recorded in our favor and remain a source of benefit to us all. We ask Allah to benefit us with the knowledge we have gained, to make us beneficial to others, and to increase us in wisdom and guidance. Indeed, He is the All-Hearing, the Responsive.

We dedicate this project to the entire Muslim Ummah. We ask Allah to bless this work, to use it in ways that please Him, and to make it sincerely for His noble face. We are confident that what is done for Allah remains, and every effort made seeking His approval will yield lasting rewards in both this world and the hereafter.

We would like to express our deepest gratitude to our beloved parents, our mother and father, for their unwavering support, love, and dedication in raising and educating us. Their prayers and care have been a continuous source of strength for us. By Allah's will and through their prayers, we have been able to overcome obstacles and achieve our goals.

We also extend our heartfelt thanks to dr. Fatima Mourad, whose invaluable support played a key role in helping us resume this project after a period of stagnation. Her guidance and wisdom were instrumental in steering us back on track. May Allah reward her generously for her kindness and support.

Our sincere thanks go to dr. Fadi Taychouri, our supervisor, for his willingness to guide us through this project. We are deeply grateful for his agreement to become our supervisor, and for his encouragement and support during the course of this work.

We would like to express our sincere appreciation to dr. Samir Mourad, Director of AECENAR, for his continued support and invaluable assistance throughout the course of this project. His guidance, generosity, and tireless efforts in providing us with the necessary resources and opportunities have been crucial in enabling us to complete this work successfully. We are deeply grateful for his contribution.

Lastly, we extend our sincere gratitude to all the esteemed doctors at the Lebanese University, who dedicated their time and effort to teaching and guiding us, despite the challenges we faced. We are especially thankful to those who supported us during this educational journey, caring for our well-being as if we were their own children. Special thanks go to dr. Rabih Dib and dr. Mohammad Abdelwahab, whose dedication, guidance, and commitment to our success have been pivotal in helping us reach this stage in our academic journey.

Abstract

This thesis explores the design and analysis of a LOX/LCH_4 thruster engine with a pressure feed system, tailored to efficiently transfer a spacecraft from Low Earth Orbit (LEO) to Geostationary Orbit (GEO). Blending innovation with practical feasibility, the study delves into advanced computational tools to optimize engine performance and sustainability.

The first phase involves calculating key performance parameters using NASA CEA and RPA software to determine the optimal oxidizer-to-fuel mixture ratio and evaluate specific impulse, effective exhaust velocity, and combustion characteristics. These findings guide the design of critical engine components, including the thrust chamber, combustion chamber, and nozzle, ensuring optimal operation under vacuum conditions for a target thrust force of 5 kN.

The second phase focuses on propellant calculations for orbital transfer, employing the Tsiolkovsky rocket equation to estimate fuel requirements based on spacecraft mass and mission Δv. Thermal management strategies are explored through RPA simulations to develop effective cooling and heat recovery systems, enhancing engine reliability and efficiency.

This research bridges the gap between theoretical propulsion models and practical design, contributing to the development of efficient and reliable liquid propulsion systems for small satellite missions. By integrating advanced simulation tools and focusing on performance optimization, the study paves the way for future advancements in sustainable and cost-effective space exploration.

Keywords: LOX/LCH_4 thruster engine, pressure feed system, NASA CEA, RPA, orbital transfer, chemical propulsion, heat recovery, space exploration.

Résumé

Cette thèse explore la conception et l'analyse d'un moteur-fusée LOX/LCH_4 avec un système d'alimentation par pression, conçu pour transférer efficacement un engin spatial de l'orbite terrestre basse (LEO) à l'orbite géostationnaire (GEO). Alliant innovation et faisabilité pratique, l'étude s'appuie sur des outils informatiques avancés pour optimiser les performances du moteur et sa durabilité.

La première phase consiste à calculer les principaux paramètres de performance à l'aide des logiciels NASA CEA et RPA afin de déterminer le rapport optimal oxydant/carburant et d'évaluer l'impulsion spécifique, la vitesse d'éjection effective et les caractéristiques de combustion. Ces résultats orientent la conception des composants clés du moteur, notamment la chambre de poussée, la chambre de combustion et la tuyère, garantissant un fonctionnement optimal dans des conditions de vide pour une poussée cible de 5 kN.

La deuxième phase se concentre sur les calculs de propergol pour le transfert orbital, en utilisant l'équation de Tsiolkovski pour estimer les besoins en carburant en fonction de la masse de l'engin spatial et du Δv de la mission. Les stratégies de gestion thermique sont étudiées à l'aide de simulations avec RPA pour développer des systèmes de refroidissement et de récupération de chaleur efficaces, améliorant ainsi la fiabilité et l'efficacité du moteur.

Cette recherche comble le fossé entre les modèles théoriques de propulsion et la conception pratique, en contribuant au développement de systèmes de propulsion liquide efficaces et fiables pour les missions de petits satellites. En intégrant des outils de simulation avancés et en mettant l'accent sur l'optimisation des performances, cette étude ouvre la voie à de futures avancées dans l'exploration spatiale durable et rentable.

Mots-clés: moteur-fusée LOX/LCH_4, système d'alimentation par pression, NASA CEA, RPA, transfert orbital, propulsion chimique, récupération de chaleur, exploration spatiale.

Abbreviations

LOX	Liquid Oxygen
LCH_4	Liquid Methane
LEO	Low Earth Orbit
GEO	Geostationary Orbit
CEA	Chemical Equilibrium with Applications
NASA	National Aeronautics and Space Administration
RPA	Rocket Propulsion Analysis
CAE	Computer-Aided Engineering (tools)

List of Parameters

MR	Oxidizer-to-Fuel Ratio
P_C	Combustion Chamber Pressure
p_e	Exit Pressure
p_a	Ambient Pressure
Isp	Specific Impulse
C_f	Thrust Coefficient
γ	specific heat ratio of gas
a	Sonic Velocity
h	Enthalpy
s	Entropy
G	Gibbs Energy
u	Internal Energy
C_p	Specific Heat at Constant Pressure
T	temperature
c	Effective Exhaust Velocity
V_e	Exit velocity
g	gravitational acceleration
$\dot{m}$	Total Propellant Mass Flow Rate
$\dot{m}_{CH4}$	Fuel Mass Flow Rate
$\dot{m}_{O2}$	Oxidizer Mass Flow Rate
F	Thrust Force
C^*	Characteristic velocity
A_t	Nozzle Throat Area
D_t	Nozzle Throat Diameter
A_e	Nozzle Exit Area
D_e	Nozzle Exit Diameter
A_C	Combustion Chamber Area
D_C	Combustion Chamber Diameter
V_C	Combustion Chamber Volume
L_C	Combustion Chamber Length
L^*	Characteristic length of the Combustion Chamber
ε	Nozzle Expansion Ratio
t_S	Propellant Stay Time
v	specific volume of propellant

R	specific gas constant
R_U	universal gas constant
MW	Molecular Weight
Δv	velocity change
ρ_{LO2}	Liquid Oxygen Density
ρ_{LCH4}	Liquid Methane Density
m_i	Initial mass (spacecraft mass including fuel)
m_f	Final mass (spacecraft mass without fuel)
M_{LO2}	Oxidizer Mass
M_{LCH4}	Fuel Mass
V_{LO2}	Liquid Oxygen Volume
V_{LCH4}	Liquid Methane Volume
t_b	Burn Time
hc1, hc min, hc2	Rib Height
a1, a min, a2	Channel Width
b1, b min, b2	Rib Width
T_{wg}	Temperature of chamber wall on its hot gas side
T_{wi}	Temperature between the thermal barrier coating layer and chamber wall
T_{wc}	Temperature of chamber wall on its cooler side
T_c	Temperature of the coolant
p_c	Pressure of the coolant
w_c	Velocity of the coolant
ρ	Density of the coolant
q_{conv}	Convective Heat Flux
q_{rad}	Radiative Heat Flux
q_{total}	Total Heat Flux
h	Heat Transfer Coefficient
T_{gas}	combustion gas temperature
T_{wall}	inner wall temperature
ϵ	Emissivity
σ	Stefan-Boltzmann constant
T_m	Melting temperature at standard pressure
Δv	Change in specific volume during melting
ΔH_f	Latent heat of fusion
$T_m^{'}$	Melting temperature at combustion chamber pressure

List of Tables

List of Equations

List of Figures

Table of contents

1 Introduction

1.1 Overview of the Thruster Design Process

The goal of this thesis is to design a LOX/LCH4 thruster engine with a pressure feed system for transferring spacecraft from Low Earth Orbit (LEO) to Geostationary Earth Orbit (GEO), with an integrated heat recovery system. The process of designing this thruster engine requires a comprehensive approach that takes into account performance, efficiency, and reliability, while adhering to mission-specific constraints such as weight, size, and thermal management. This chapter introduces the methodology followed in this project, covering the mission requirements, design constraints, and key performance metrics used in the development of the engine.

The design approach is broken down into several key stages, from identifying mission objectives to finalizing the components and conducting structural and thermal analyses using computational tools like RPA.

1.2 Methodology for Thruster Development

The development of the LOX/LCH_4 thruster engine follows a structured methodology tailored to meet the mission requirements of transferring a spacecraft from Low Earth Orbit (LEO) to Geostationary Earth Orbit (GEO). The design process balances performance optimization with constraints on weight, size, and operational efficiency.

1.2.1 Design Requirements and Constraints

The development of the LOX/LCH4 thruster engine is driven by specific mission requirements, particularly the need to provide efficient thrust while keeping the system compact and reliable. This section highlights the major design requirements and the operational constraints that shape the thruster engine's development.

1.2.1.1 Mission Requirements

The mission objective is to transfer a spacecraft from Low Earth Orbit (LEO) to Geostationary Earth Orbit (GEO) using a LOX/LCH_4 propulsion system. To achieve this, the design must fulfill the following key requirements:

1. Payload and Dry Mass Specifications:

- Payload mass: 50 kg
- Dry mass of the spacecraft: 60 kg

2. Δv Requirement:

- The orbit transfer maneuver requires achieving the necessary Δv, accounting for gravitational and orbital mechanics considerations.

3. Thrust Force:

- The propulsion system should generate sufficient thrust to efficiently perform the orbit transfer. An estimated thrust of 5 kN is considered as a preliminary target.

4. Propellant Selection and Mixture Ratio:

- Propellants: Liquid Oxygen (LOX) and Liquid Methane (LCH_4) are chosen for their performance characteristics, storability, and environmental compatibility.
- The oxidizer-to-fuel ratio will be optimized in later calculations to achieve maximum engine performance.

5. Structural and Thermal Design:

- The engine must be capable of withstanding high-pressure combustion and extreme thermal conditions, necessitating robust materials and an efficient cooling system.

6. System Integration:

- The propulsion system design must ensure seamless integration with the spacecraft, adhering to constraints on mass, volume, and structural compatibility.

These mission requirements establish the foundation for the propulsion system's design and performance objectives, guiding subsequent calculations and optimization efforts.

1.2.1.2 Performance Metrics

Key performance metrics are defined to evaluate the effectiveness of the thruster engine:

- Specific Impulse (Isp): This is a key measure of fuel efficiency, which the engine design aims to maximize while maintaining consistent combustion.
- Thrust-to-Weight Ratio: A high thrust-to-weight ratio is targeted to provide optimal performance without adding unnecessary mass to the spacecraft.

1.2.1.3 Physical and Operational Constraints

Key constraints influencing the design include:

- Weight and Size: Minimizing engine mass and volume to fit within spacecraft constraints.
- Pressure and Temperature: The engine operates at high chamber pressures, estimated at 300 psia (approximately 20.7 bar), and temperatures exceeding 3000 K, requiring robust materials and precision engineering.
- Thermal Management: Incorporating reliable cooling systems to handle extreme heat and improve efficiency through heat recovery.

1.2.1.4 Design Challenges

The engine design faces several challenges:

- Thermal Stress: High temperatures in the combustion chamber and nozzle require advanced cooling techniques and heat-resistant materials.
- Pressure Stability: Ensuring stable chamber pressure without pumps poses a challenge to achieving consistent thrust.
- Efficient Combustion: The thruster must ensure complete and efficient combustion of LOX and LCH4 to maximize performance while minimizing fuel consumption.

1.2.2 Combustion Chamber Design

The combustion chamber is a crucial component responsible for igniting and sustaining the combustion process. Its design must ensure efficient combustion while managing extreme temperature and pressure conditions. The following aspects are considered in the design:

- Chamber Geometry: The combustion chamber’s geometry, is optimized for fuel mixing and complete combustion.
- Material Selection: Materials like Inconel or copper alloys are selected for their strength under high thermal and mechanical stress.
- Cooling System: Regenerative cooling ensures thermal stability.

1.2.3 Nozzle Design

The nozzle transforms thermal energy into kinetic energy to produce thrust:

- Geometry: Optimized throat and exit diameters maximize exhaust velocity.
- Materials: High-temperature-resistant materials ensure durability.
- Cooling Requirements: Regenerative cooling is integrated for thermal management.

1.2.4 Pressure Feed System

A pressure feed system is chosen for its simplicity and reliability compared to pump-fed systems. Key considerations include:

- Feed System Overview: The pressure feed system eliminates the need for complex pumps, reducing system mass and complexity.
- Tank Design: Propellant tanks are designed to withstand high pressures and provide steady flow into the combustion chamber.
- Pressurization Gas: Helium is used for pressurizing the tanks due to its inert nature and light weight.

1.2.5 Cooling and Heat Recovery System

Effective cooling and heat recovery are vital to ensure long engine life and improve efficiency:

- Cooling Techniques: Regenerative cooling is implemented, where the fuel is used to cool the combustion chamber walls before injection.
- Heat Recovery: The system recovers heat from the combustion process to preheat the fuel, improving the overall efficiency of the engine.

1.2.6 Structural and Thermal Analysis

To ensure the engine's reliability under operational conditions, structural and thermal analyses are essential:

- RPA: Computational analysis tools like RPA are used to simulate thermal stresses, fluid dynamics, and heat transfer in the thruster engine.

2 Fundamentals of Thruster Propulsion

2.1 LEO to GEO Transfer

2.1.1 Low Earth Orbit (LEO)

Low Earth Orbit (LEO) refers to an orbit around the Earth with an altitude typically ranging from 160 km to 2,000 km. This region is commonly used for various satellite missions, including communications, Earth observation, and human spaceflight, due to its proximity to the Earth's surface, which allows for lower launch costs and shorter orbital periods.

For the spacecraft in this project, LEO represents the point of departure, from which the thruster engine will provide the necessary delta-v to execute the transfer to GEO, fulfilling the mission's orbital transfer objectives.

2.1.2 Geostationary Earth Orbit (GEO)

The geostationary orbit (GEO) is a circular orbit located approximately 35,786 kilometers (22,236 miles) above the Earth's equator, where a satellite's orbital period matches the Earth's 24-hour rotation. This synchronization results in the satellite appearing stationary to an observer on the ground, continuously covering the same geographical area. This stable positioning is invaluable for communication satellites, weather monitoring, and other applications that require uninterrupted coverage of specific regions.

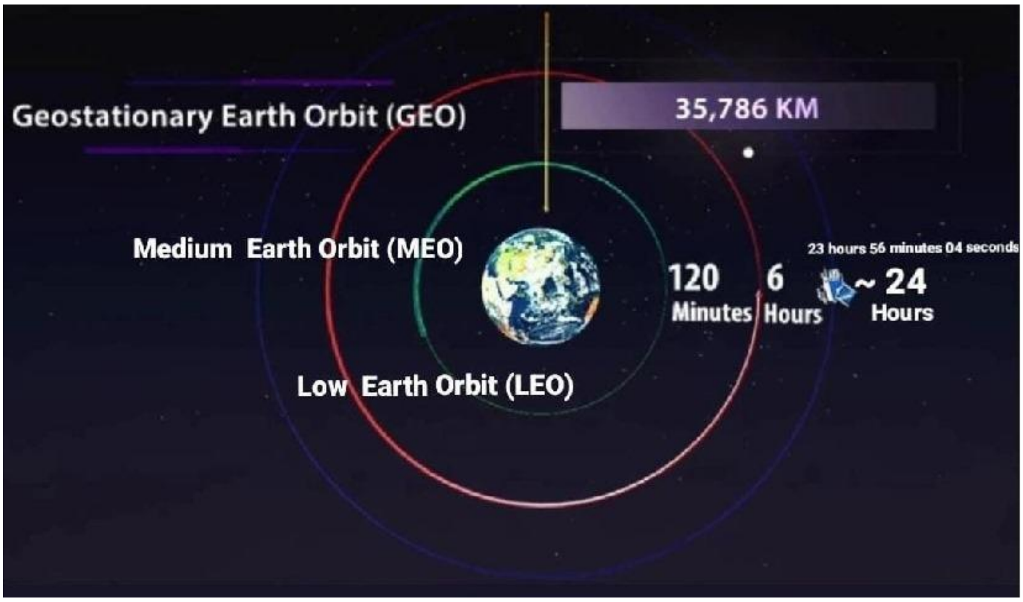

Figure 2.1 illustration of Orbital Altitudes: Low Earth Orbit (LEO), Medium Earth Orbit (MEO), and Geostationary Earth Orbit (GEO)

2.1.2.1 Importance of the Geostationary Orbit

- **Continuous Coverage:** GEO satellites provide uninterrupted communication and monitoring over large regions, which is crucial for services like television broadcasting, telecommunications, and emergency responses.

- **Simplified Ground Equipment:** Since satellites in GEO remain fixed relative to Earth's surface, ground-based antennas can stay pointed in a single direction, eliminating the need for complex tracking systems.
- **Improved Signal Quality:** The stable position of GEO satellites ensures stronger and more reliable signal transmission, making them ideal for high-demand applications like satellite internet and real-time communication.

2.1.3 Challenges of Direct GEO Transfers

Placing a satellite directly into GEO is challenging due to the high altitude and the energy required. Direct transport to GEO is rarely practiced for the following reasons:

- **High Energy Requirements:** The altitude of GEO demands significant energy to overcome Earth's gravity and achieve the necessary orbital speed.
- **Launch Vehicle Limitations:** Most thrusters are designed to place payloads in low Earth orbit (LEO) or medium Earth orbit (MEO), making direct launches to GEO complex and expensive.
- **Gravity Losses:** A direct ascent to GEO would result in greater gravity losses, making the mission less efficient.

2.1.4 LEO to GEO Transfer Process

Given these challenges, satellites are typically launched into low Earth orbit (LEO) first. Satellites in LEO travel at high speeds, orbiting the Earth approximately every 90 to 120 minutes. This proximity allows for high-resolution imaging and low-latency communication but requires multiple satellites to cover a larger area due to their limited field of view.

Here's how the transfer process works:

- **Launch to LEO:** The satellite is initially placed in LEO, an altitude of around 160 to 2,000 kilometers, where launching is easier and requires less energy.
- **Transfer to GTO:** From LEO, the satellite is moved into a geostationary transfer orbit (GTO), an elliptical orbit with an apogee at GEO altitude. This is done using the thruster's upper stage or a separate propulsion system.
- **Final Maneuver to GEO:** At the apogee of GTO, the satellite’s propulsion system is fired to circularize the orbit, completing the transition to GEO.

2.2 Classifications Of Propulsive Devices

In the past century, a range of propulsive devices were developed for modern aircraft and spacecraft, classified into air-breathing and non-air-breathing engines (see Figure 2.2). Air-breathing engines use ambient air as an oxidizer and include gas turbines (turbojet, turbofan, turboprop), ramjets, and specialized scramjets. Non-air-breathing engines, or thruster engines, carry their oxidizer onboard and are categorized into chemical (solid, liquid, hybrid) and non-chemical (solar, electric, nuclear) types. This report focuses on chemical propulsion, with an emphasis on liquid propellant thruster engines.

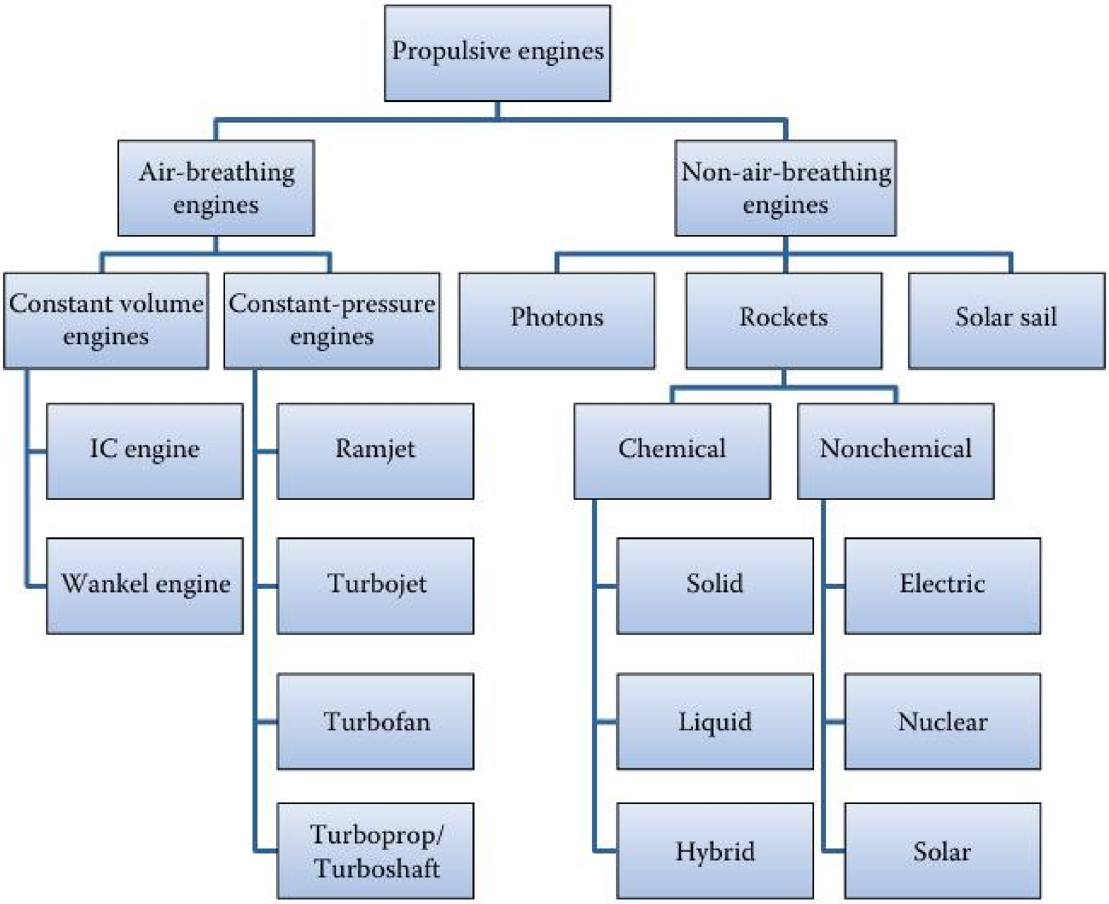

Figure 2.2 Classification of propulsive

2.3 Liquid Propellant Thrusters

Liquid propellant thruster engines have been extensively researched since the late 1930s and remain the most widely used propulsion system for space launch systems. They provide higher thrust and specific impulse due to the high chemical energy stored in liquid propellants. These engines use a liquid oxidizer and liquid fuel, which are fed into a combustion chamber either through pressurized tanks or pumps. The chemical reaction between the propellants generates hot gases that are ejected through a nozzle at high velocity, producing the necessary thrust to propel the vehicle. As the technology has matured, current developments focus on achieving design flexibility, simplicity, and reliability, all while maintaining high performance.

2.3.1 Components Of Liquid Propellant Thruster Engines

A typical liquid propellant thruster engine consists of several key components: the thrust chamber (which includes the combustion chamber and nozzle), injector, igniter, propellant tanks, propellant feed system, and cooling system (see Figure 2.3). The combustion chamber houses injectors that atomize the liquid propellants, mix them, and ignite them, resulting in the production of high-temperature, high-pressure gases. These gases are then expanded through a convergent-divergent nozzle to produce thrust.

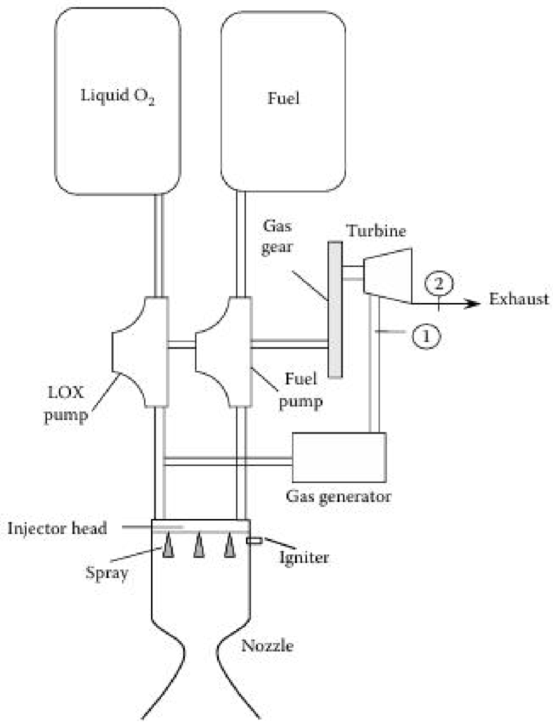

Figure 2.3 A typical liquid-propellant Thruster engine.

The propellant feed system, which may use high-pressure tanks or turbo-pumps, ensures the proper delivery of fuel and oxidizer to the combustion chamber. Efficient combustion requires the propellants to be vaporized and mixed thoroughly, which is achieved by feeding them at high pressure into the injectors. The ignition system provides the initial energy to start combustion, although hypergolic propellants ignite on contact and do not need an igniter. Finally, a cooling system is employed to manage the high temperatures in the combustion chamber and nozzle.

2.3.2 Types of Liquid-Propellant Thruster Engines

Since the development of liquid-propellant thruster engines in 1926, several variations have emerged. These engines can be broadly classified into two main types based on the number of liquid propellants used:(1) monopropellant thruster engine and (2) bipropellant thruster engine.

2.3.2.1 Monopropellant Thruster Engines

In a monopropellant thruster engine, a single liquid propellant is used, which decomposes with the help of a catalyst to produce hot gases. These gases are expanded through a nozzle to generate thrust. The key advantage of this system is its simplicity, as it eliminates the need for an oxidizer, making the overall engine design more straightforward. However, monopropellant engines are generally limited to applications requiring low thrust and short-duration burns.

A schematic of a typical monopropellant thruster engine is shown in Figure 2.4 , in which liquid propellant is injected into a catalyst bed and decomposes into high-pressure and high-temperature gas. This gas is then expanded through a convergent-divergent nozzle to create the required thrust. Monopropellants are usually chemicals that decompose easily in an exothermic reaction, releasing hot gas.

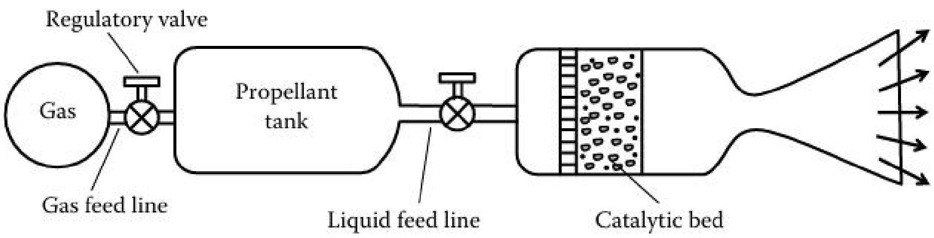

Figure 2.4 Schematic of monopropellant LPR engine.

2.3.2.2 Bipropellant Thruster Engines

Bipropellant thruster engines utilize two separate liquid propellants: one as fuel and the other as an oxidizer. This configuration, as illustrated in Figure 2.5, offers significant advantages over monopropellant engines, including higher specific impulse (performance), the ability to restart, variable thrust, and broader operational versatility. These engines are widely used in applications such as launch vehicles and missiles due to their superior performance.

A typical bipropellant thruster engine consists of has thrust chamber, injection system, cooling system, propellant feed sys tem, nozzle, and so on. The liquid fuel and oxidizer are atomized into fine sprays, mixed, vaporized, and ignited to produce high-temperature, high-pressure gases. These gases are then expanded through a convergent–divergent nozzle to generate thrust.

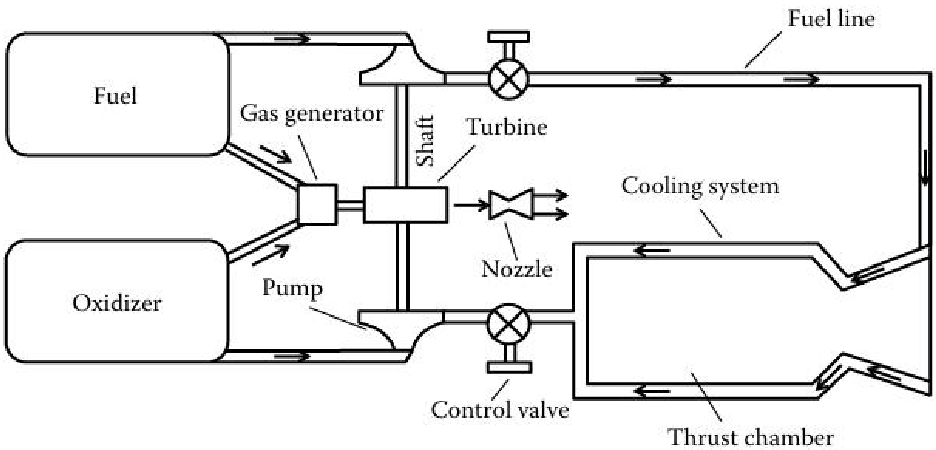

Figure 2.5 Schematic of bipropellant LPR engine.

Based on ignition methods, bipropellant engines are divided into two categories:

- **Hypergolic Engines**

In hypergolic engines, the fuel and oxidizer ignite spontaneously upon contact without the need for external ignition. Common hypergolic propellants include:

Fuels: Aniline, Triethylamine, Hydrazine, MMDH (Monomethylhydrazine), UDMH (Unsymmetrical Dimethylhydrazine)

Oxidizers: White fuming nitric acid (with nitrogen tetroxide), Red fuming nitric acid (with higher nitrogen tetroxide content)

These propellants can typically be stored at normal pressure and temperature, but some combinations, like liquid fluorine and liquid hydrogen, require cryogenic storage.

- **Non-Hypergolic Engines**

Non-hypergolic engines require external ignition energy to initiate combustion. These engines use fuels such as kerosene, hydrocarbons, alcohol, methane, and liquid hydrogen. Liquid methane (LCH4) is increasingly being favored in modern designs, especially when paired with liquid oxygen (LOX), due to its higher specific impulse, cleaner combustion, and cryogenic properties, which are easier to manage compared to liquid hydrogen.

2.3.3 Propellant Feed System

The propellant feed system plays a critical role in liquid thruster engines by delivering propellants from storage tanks to the combustion chamber at the correct flow rate and pressure. The feed system has two principal functions:

1. To increase the pressure of the propellants.

2. To supply them at design mass flow rates to the thrust chamber(s).

The energy for these functions is provided either by high-pressure gas, centrifugal pumps, or a combination of both. The choice of a specific feed system is governed by the thruster application, mission duration, number and type of thrust chambers, past experience, and general design requirements such as simplicity, ease of manufacture, cost-efficiency, and minimum inert mass.

Feed systems consist of components such as piping, valves, provisions for filling, draining, filters, and control devices to manage propellant flow. Depending on how the propellants are pressurized and fed into the thrust chamber, the feed system is classified as pressure-fed or pump-fed as shown in Figure 2.6.

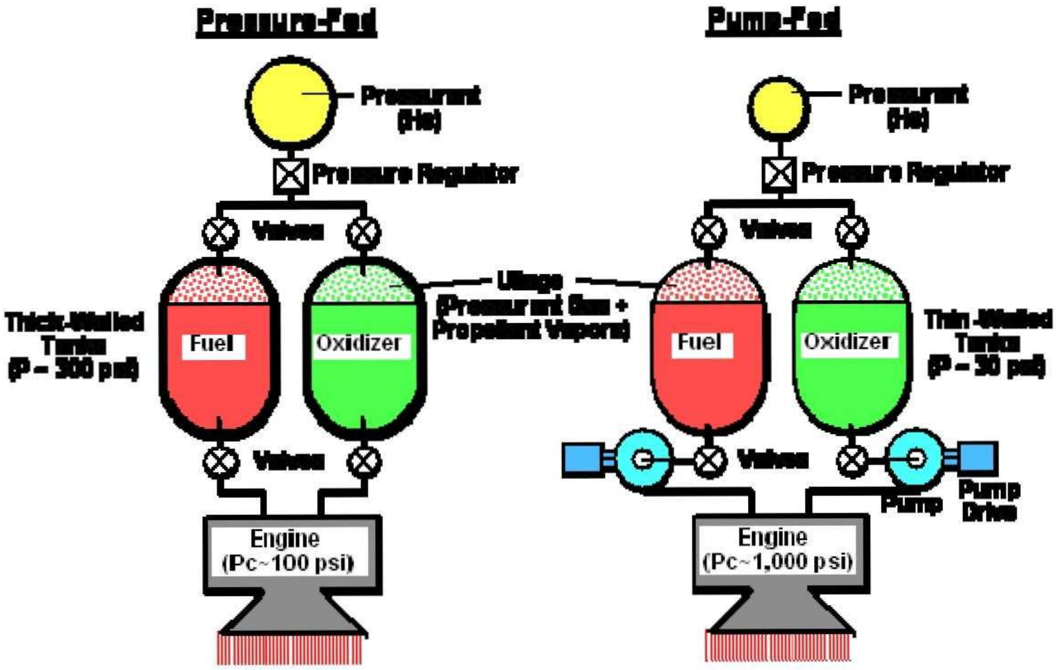

Figure 2.6 Pressure-Fed and Pump-Fed Liquid Propulsion

2.3.3.1 Pressure Feed System

The pressure feed system uses high-pressure gas to force the propellants from the tanks into the combustion chamber. This type of system is suitable for low-thrust applications with low chamber pressures and relatively low total impulse, such as attitude control systems or small upper stages.

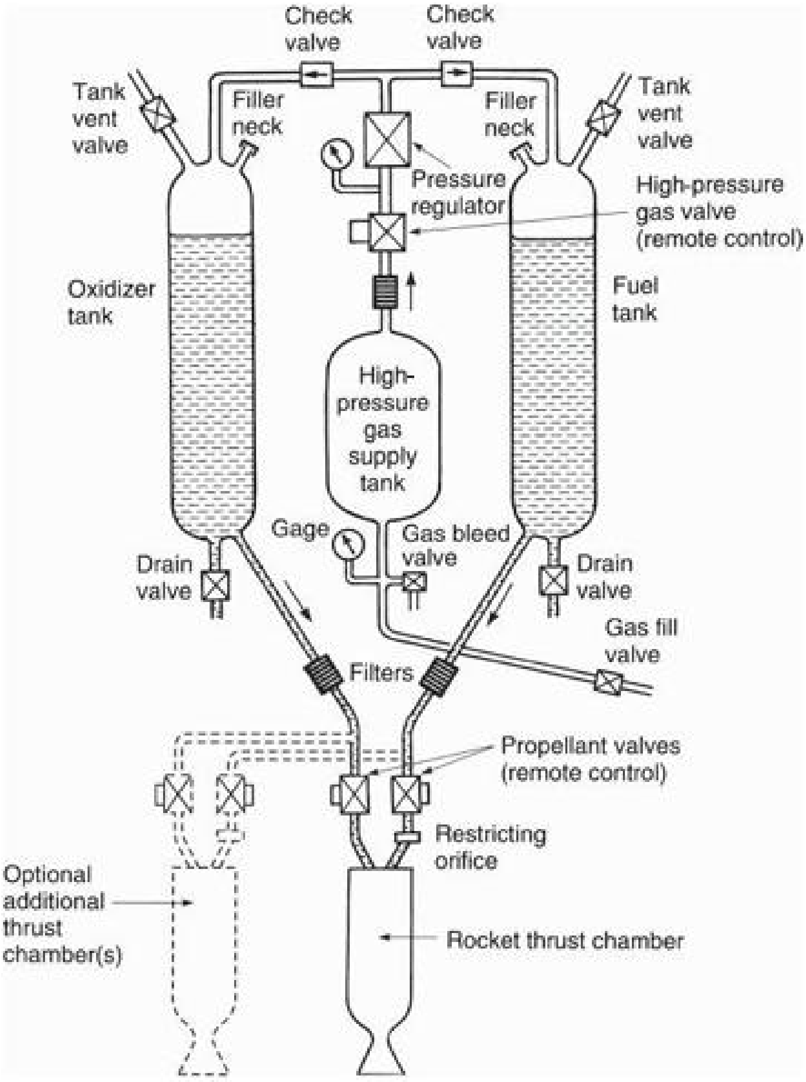

Figure 2.7 Schematic Flow Diagram of a Liquid Propellant Thruster Engine with a Gas Pressure Feed System.

The system typically includes the following components: (see Figure 2.7)

- Pressurized gas tank: Stores the high-pressure gas.
- Pressurant gas or other expulsion devices (e.g., helium gas) to provide the energy for the feed system
- Valves to control the pressure and flow and filters.
- Ducting or piping to transfer fluids to the combustion chamber.
- Thrust chamber: Converts the propellants' energy into thrust.
- Gas pressure regulator: Manages the pressurant gas flow to maintain consistent pressure.
- Propellant tanks: Hold the fuel and oxidizer.
- Propellant valves and feed lines: Direct propellant flow into the thrust chamber.

These systems are generally classified according to the source of the pressurant gas, which determines how the propellants are expelled from the tanks. There are two common configurations:

- **Monopropellant systems**, where a single propellant, such as hydrazine, flows through a catalyst bed and expands in a nozzle to generate thrust.
- **Bipropellant systems**, which use separate oxidizer and fuel tanks, both requiring a pressurization system to expel the propellants into the feed lines and ultimately to the thrust chamber.

One of the advantages of pressure-fed systems is their simplicity and reliability. These systems are often used in applications with low to moderate engine performance requirements, such as orbital maneuvering, reaction control, and small upper-stage propulsion. However, they tend to be heavier due to the need for thick-walled pressurized tanks.

Stored-gas pressurant systems are widely used, where gases such as helium (due to its low molecular weight) are stored at high pressures (up to 270 atm) and then supplied to the propellant tanks at regulated pressures. Factors that influence the selection of pressurization gases include mission requirements, cost, weight, reliability, and compatibility with tank materials.

The pressure-fed system is favored when system simplicity and low cost are prioritized over performance. Nonetheless, these systems are typically heavier because of the need for thick-walled, pressurized propellant tanks.

2.3.3.2 Turbopump Feed System

The turbo-pump feed system is favored for high-thrust, long-duration thruster engine systems with high specific impulse, as the gas pressure feed system is unsuitable for such applications. Turbo-pump systems are typically used in boosters, sustainers of space vehicles, long-range missile systems, and aircraft performance augmentation due to their advantages over gas pressure feed systems, such as:

- Flexibility: Easier control of pump speed allows better operational flexibility.
- High Pressure: The system can achieve stable pressures as high as 6–8 MPa.
- Compact Design: Smaller volume requirements, even for higher-thrust engines.
- High Power-to-Weight Ratio: Ranges from 15 to 50 kW/kg, making it more efficient.

A simplified turbo-pump system consists of several key components: (see Figure 2.8)

- Propellant tanks
- Inlet and discharge ducts
- Pumps: Pressurize the propellants.
- Turbine: Powers the pumps.
- Speed reduction gearbox: Transfers torque from the turbine to the pump at a reduced rotational speed.
- Gas generator: Produces hot gases by burning a small portion (1%-5%) of the total propellant flow, which powers the turbine.
- Heat exchanger and nozzle: Expands the hot gases generated by the gas generator.

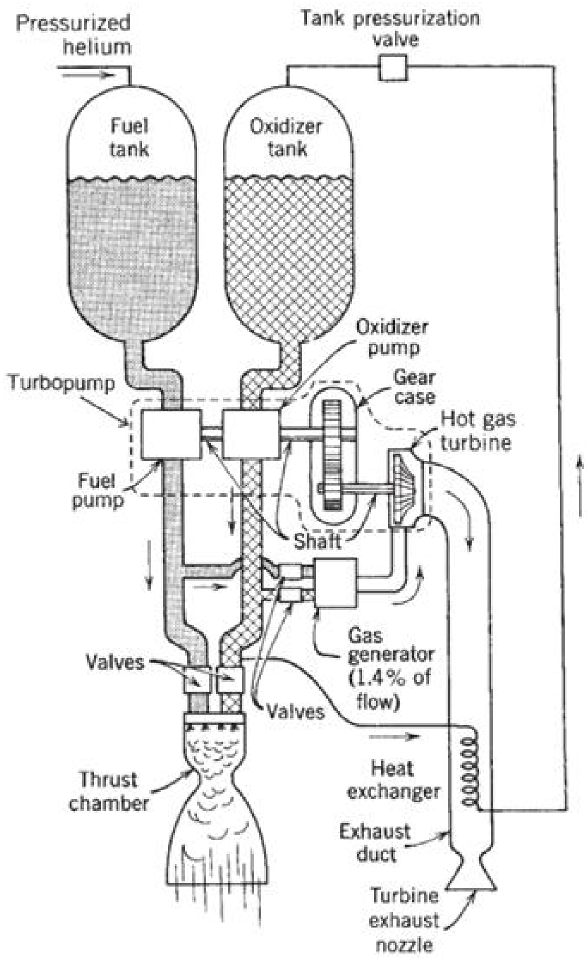

Figure 2.8 Simplified Schematic Diagram of a Liquid Propellant Thruster Engine with a Turbopump Feed System and Separate Gas Generator.

In this system, propellants are pressurized by pumps driven by turbines. The turbines are powered by hot gases, which are created in the gas generator by combusting a small fraction of the propellant. This setup allows the turbo-pump system to deliver high performance, making it ideal for demanding missions where weight and engine efficiency are critical.

Turbo-pump feed systems are classified based on the configuration of the turbine-pump drive and the exhaust gas discharge modes. The main types include:

1. Monopropellant Cycle

2. Bipropellant Cycle

3. Expander Cycle

4. Staged Combustion Cycle

2.4 Liquid Propellants

Propellants, the working substances of thruster engines, constitute the fluid that undergoes chemical and thermodynamic changes. The term "liquid propellant" encompasses all the various propellants stored as liquids.

Liquid propellants consist of a liquid fuel, a liquid oxidizer, and sometimes liquid additives. Examples of liquid fuels include hydrocarbons, liquid hydrogen, and alcohols, while common oxidizers are liquid oxygen, nitric acid, and liquid fluorine.

Liquid propellants can be classified based on several factors such as fuel-oxidizer arrangement, energy content, ignitability, and storability. Broadly, they are categorized into:

2.4.1 Monopropellants

Monopropellants are further divided into:

- **Simple Monopropellants:** The fuel and oxidizer are part of the same molecule, such as in methyl nitrate (CH_3NO_3), which decomposes into CH_3O and NO_2.
- **Composite Monopropellants:** A mixture of fuel and oxidizer, such as nitric acid and amyl acetate, which undergo exothermic reactions.

2.4.2 Bipropellants

Bipropellants can be further classified based on ignitability into:

- **Hypergolic Propellants**
- **Non-Hypergolic Propellants**

2.4.3 Energy Classification

Liquid propellants are also categorized by energy content, which typically correlates with their specific impulse. They are divided into:

- **Low-Energy Propellants:** These have lower specific impulses and are used for simpler applications.
- **Medium-Energy Propellants:** Offering a balance between performance and complexity.
- **High-Energy Propellants:** Known for delivering high specific impulses, such as hydrogen-fluorine (H_2/F_2) and liquid hydrogen-liquid oxygen (LH_2/LOX).

The choice of liquid propellants depends on the mission requirements, such as performance, storability, and safety, making them highly versatile for various thruster propulsion applications.

2.4.4 Why LOX / LCH4 ?

The development of LOX/LCH4 propulsion technology has a rich history, dating back to the 1970s. Efforts during this period focused on creating technologies to store and utilize cryogenic propellants in space as a non-toxic alternative to traditional propellants, aiming to achieve high-performance spacecraft. Numerous programs explored non-toxic propellants suitable for spacecraft thrusters, including liquid hydrogen and liquid oxygen. However, using liquid hydrogen for propulsion proved to be complicated due to challenges in long-term storage and the necessity for engine pumps. The high boil-off rate of hydrogen, the large volume of storage tanks, and the complexity of redundant pump systems led to increased spacecraft mass and costs, which counteracted the advantages of high specific impulse offered by the H2/O2 combination. While LO2/LH2 performs well for short-duration upper stages, denser propellants are more favorable for smaller, long-duration spacecraft.

In the 1980s, liquid methane emerged as a superior hydrocarbon fuel for in-space applications, thanks to its clean-burning properties, non-sooting characteristics, compatibility with LO2, and ability to be pressure-fed. LOX/LCH4 outperforms hydrazine and electric propulsion systems in thrust capability and is recognized as a green propellant ideal for deep space missions and planetary landers, offering increased cargo capacity and high thrust along with substantial delta-V capabilities.

Methane/oxygen thruster engines offer potentially significant life cycle mission advantages compared to traditional thruster propellants used in the United States today. Figure 2.9 shows that liquid methane (LCH4) and liquid oxygen (LOX) propulsion is very competitive based on bulk density impulse compared to current booster and in-space propellant combinations traditionally used today.

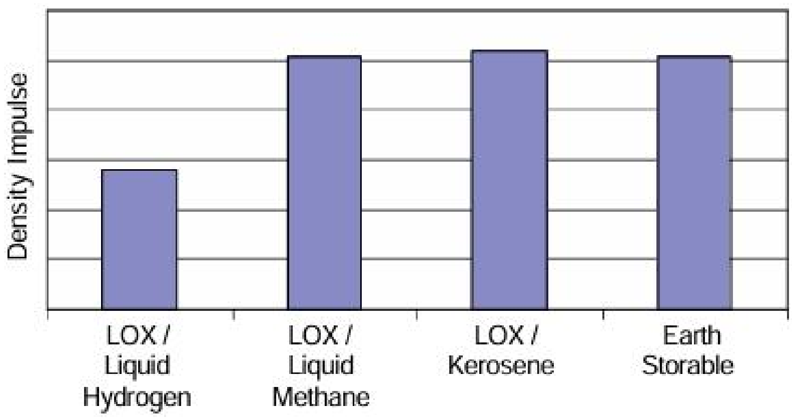

Figure 2.9 Density impulse Comparisons show methane comparable with traditional propellants.

The combination of LOX and LCH4 can significantly reduce spacecraft mass due to its higher specific impulse (Isp) when used with composite propellant tanks and cold-stored gaseous helium (GHe) pressurant. LOX/LCH4 is storable in space without requiring heaters like earth-storable propellants or active cooling like LH2. In certain environments, LOX and methane can be stored indefinitely at temperatures ranging from 90 to 120 K in deep space or for months in other orbits.

Additionally, LOX/LCH4 offers key reliability advantages for spacecraft propulsion. LOX is compatible with many materials, while methane is compatible with nearly all materials, and both are non-corrosive. The pressure-fed capability of LOX/LCH4 enhances reliability compared to LOX/LH2, which typically requires pump-fed systems.

These clean-burning, high vapor pressure propellants do not contaminate sensitive optics or damage surfaces, which is beneficial for platforms such as the International Space Station. Ground operations see significant improvements with LOX/LCH4, as these propellants are non-toxic and low-cost, facilitating rapid loading, testing, reusability, and clean turnaround operations for spacecraft and subsystems. Automated loading of spacecraft can occur concurrently with the launch vehicle, similar to LOX/LH2 upper stages, but without the complications of LH2 air liquefaction or toxic propellant issues. There is no need for hazardous propellant pre-loading at offsite facilities, allowing inert spacecraft to be transported and integrated with the launch vehicle easily. For launch pad operations, mobile propellant storage tanks, transfer lines, and cryogenic fluid couplings are necessary. The high vapor pressure of both propellants significantly enhances reusability, as they can be easily and safely inerted with GN2 and vented.

2.5 Propellant Tanks and Pressurization

In liquid bipropellant thruster engine systems, the propellants are stored in separate oxidizer and fuel tanks within the vehicle. Monopropellant thruster engines, by definition, use only one propellant tank. Typically, one or more high-pressure auxiliary gas tanks are included, which are used to pressurize the propellant tanks. However, there are tank pressurization methods that utilize heated gas from the engine, eliminating the need for additional heavy, high-pressure gas storage tanks.

The arrangement of tanks can vary, and the design, shape, and placement of the tanks can influence the vehicle's center of gravity. Typical arrangements are illustrated in Figure 2.10. Since propellant tanks must also fly, their mass is a significant factor, and they are often highly stressed. Common tank materials include aluminum, stainless steel, titanium, alloy steels, and fiber-reinforced plastics with a thin, impervious metal liner to prevent leakage through the porous walls of the fiber-reinforced material.

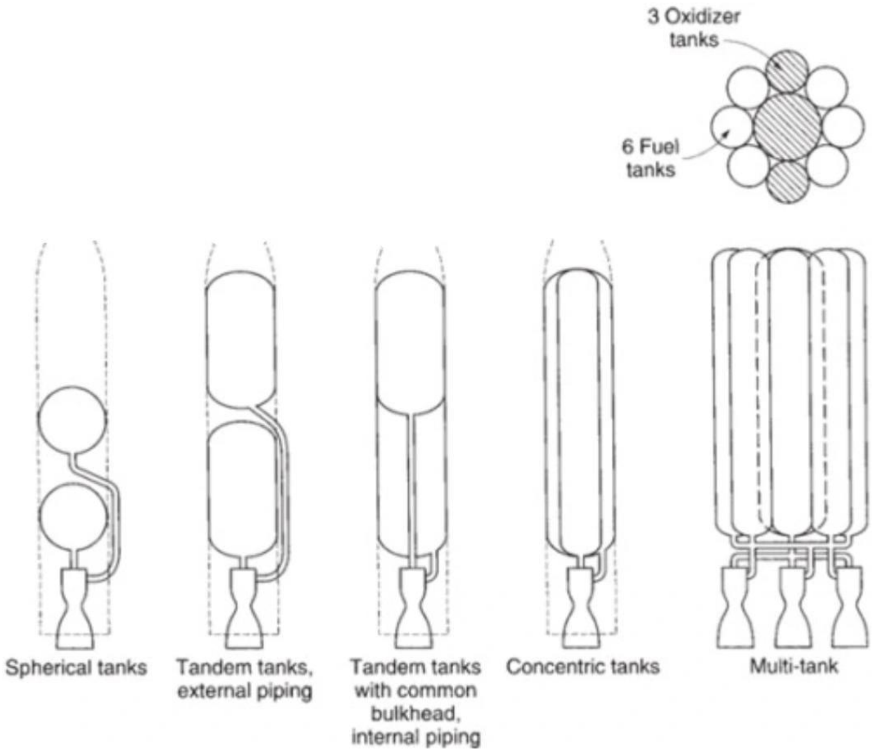

Figure 2.10 Simplified Sketches of Typical Tank Arrangements for Large Turbopump-Fed Liquid Bipropellant Thruster Engines.

The optimal shape for both propellant and gas pressurizing tanks is spherical, as this shape results in the least mass for a given volume. Small spherical tanks are often used in reaction control engine systems, where they can be easily integrated with other vehicle equipment. However, larger spherical tanks, which are necessary for primary propulsion systems, do not efficiently fill the available space in the vehicle. Therefore, larger tanks are often integrated into the vehicle's fuselage or wings, typically cylindrical with hemispherical or ellipsoidal ends, but they can also be irregular in shape.

There are several categories of tanks in liquid propellant propulsion systems, with relevant pressure values generally falling into the following:

- **Pressurized feed systems:** Propellant tanks in these systems typically operate at average pressures between 1.3 and 9 MPa (200 to 1800 psi). These tanks have thick walls and are relatively heavy.
- **High-pressure stored gas tanks:** Used to expel propellants, these tanks need to withstand pressures between 6.9 and 69 MPa (1000 to 10,000 psi). They are usually spherical to minimize inert mass, and several small spherical tanks may be connected together. In some vehicles, these smaller high-pressure gas tanks are placed inside the liquid propellant tanks.
- **Turbopump feed systems:** The propellant tanks in these systems must be pressurized slightly (to prevent pump cavitation) to average pressures between 0.07 and 0.34 MPa (10 to 50 psi). These low pressures allow for thinner tank walls, resulting in lower inert tank mass for turbopump feed systems.

2.5.1 Tank Pressurization

As previously mentioned, the objective of feed systems is to move propellants under pressure from propellant tanks to the thrust chamber(s). The tank pressurization system is the part of the feed system that provides the propellant expellant gas.

2.5.1.1 Types of Tank Pressurization Systems:

- **Pressurized Gas Feed System:** A relatively high-pressure gas displaces the propellants from the tanks.
- **Pumped Feed System:** The main energy for feeding the propellants comes from one or more pumps. This system requires lower gas pressures in the tanks to move the propellants to the pump inlet, helping to avoid pump cavitation.

2.5.1.2 Sources of Pressurizing Gas Used in Tank Pressurization Systems:

- **High-Pressure Inert Gases:** Commonly used gases include helium, nitrogen, and air, stored at ambient temperature. When gases expand adiabatically, their temperature drops.
- **Heated High-Pressure Inert Gases:** Typically heated to between 200 and 800 °F (93 to 427 °C), which reduces the amount of required gas and thus the inert mass of the pressurizing system. Examples include gases heated by a heat exchanger using warm exhaust from a gas generator or turbine.
- **Gases Created by Chemical Reactions:** These can be derived from either liquid bipropellants, monopropellants, or solid propellants, resulting in “warm gas.” The term “warm gas” typically refers to gases between 400 and 1600 °F (204 to 871 °C), distinguishing it from the “hot gas” in the main combustion chamber (4000 to 6000 °F or 2204 to 3319 °C). Chemically generated warm gases usually result in lighter tank pressurization systems compared to heated inert gas systems.
- **Evaporated Flow of Cryogenic Liquid Propellant:** A small portion of cryogenic liquid propellant, usually liquid hydrogen or liquid oxygen, can be evaporated by applying heat from a thrust chamber cooling jacket or from turbine exhaust gases, using part or all of this evaporated flow for tank pressurization.

- **Direct Injection of Hypergolic Fuel:** A small stream of hypergolic fuel can be injected into the main oxidizer tank and a small flow of hypergolic oxidizer into the fuel tank, though this has seen limited success.
- **Self-Pressurization of Cryogenic Propellants by Evaporation:** This method is feasible but can be difficult to control, with limited experience in this area.

2.5.1.3 Information Required for Designing and Analyzing a Pressurization System:

To design or analyze any pressurization system, it is necessary to have relevant information about the tank and the engine, which can include:

- Basic Engine Parameters: Such as propellant flow, thrust, duration, and pulse width.
- Propellant Tank Volume and Percent Ullage of Tank Volume.
- Storage Temperature Range.
- Properties of the Propellant and Pressurizing Gas.
- Propellant Tank Pressure and Gas Tank Pressure.
- Amount of Unavailable Residual Propellant.

2.6 Thrust Chambers

The thrust chamber is a critical component of a thruster engine, responsible for converting the chemical energy stored in the propellants into the kinetic energy needed to generate thrust. It comprises three main parts: an injector, a combustion chamber, and a nozzle.

In simple terms, the fuel and oxidizer are combined in the combustion chamber, creating high-temperature and high-pressure gases. These gases are then expanded through the nozzle, converting pressure and temperature into velocity. At the nozzle throat, the flow becomes choked thermodynamically, reaching sonic velocity. The combustion gases continue expanding at supersonic speeds through the diverging section of the nozzle. This process exchanges internal energy for kinetic energy, generating the momentum thrust required for propulsion.

This section will cover key elements associated with thrust chamber design, organized as follows: a comprehensive description of the thrust chamber is presented, detailing the underlying design concept and its applications. Then, various nozzle types used with the thrust chamber are explained.

As illustrated in Figure 2.11, the thrust chamber with an integral nozzle operates as follows: the propellants enter through the injector and undergo a series of complex physical and chemical processes such as atomization, vaporization, mixing, reaction, and expansion. The combustion chamber contains the high-pressure, high-temperature combustion gases and ensures stable combustion throughout the process. These gases are then expanded through the nozzle, with the diverging nozzle section (downstream of the throat) typically forming an integral part of the combustion chamber hardware. In many cases, a separate nozzle extension is added to further expand the gases and increase thrust.

For a liquid bi-propellant thruster engine, the combustion process can be summarized as follows:

- **Propellant Injection and Atomization:** the fuel and the oxidiser are injected into the combustion chamber at the correct oxidizer/fuel mixture ratio (O/F) and atomized into fine droplets.
- **Vaporization and Mixing:** These droplets vaporize as they absorb heat from the surrounding gases. Throughout this process, the droplets' size and velocity change, leading to rapid mixing and further heating of the vaporized propellants. The reaction between these vaporized propellants significantly increases the gaseous mass flow rate within the combustion chamber.
- **Combustion Process:** The gas-phase reactions, driven by high-speed diffusion of reactive molecules and atoms, continue as the gases flow toward the chamber throat. Combustion is generally completed upstream of the throat, ensuring that all droplets have vaporized. However, certain conditions may cause shock waves or pressure oscillations, leading to "combustion instability," which can produce destructive vibrations and heat flux. Thus, ensuring stable combustion is a significant aspect of thruster design and development.
- **Gas Acceleration and Ejection:** As the combustion products move toward and through the throat, they accelerate to sonic speeds and then to supersonic velocities within the expanding nozzle section, ultimately being expelled to generate thrust.

The principal components of a thrust chamber are the injector including the propellant inlets and distributing manifolds, the ignition device (which is necessary in case of a thruster engine burning non-hypergolic propellants), the combustion chamber, the converging portion of the nozzle between the inlet plane and the throat, and the diverging portion of the nozzle between the throat and the exit plane.

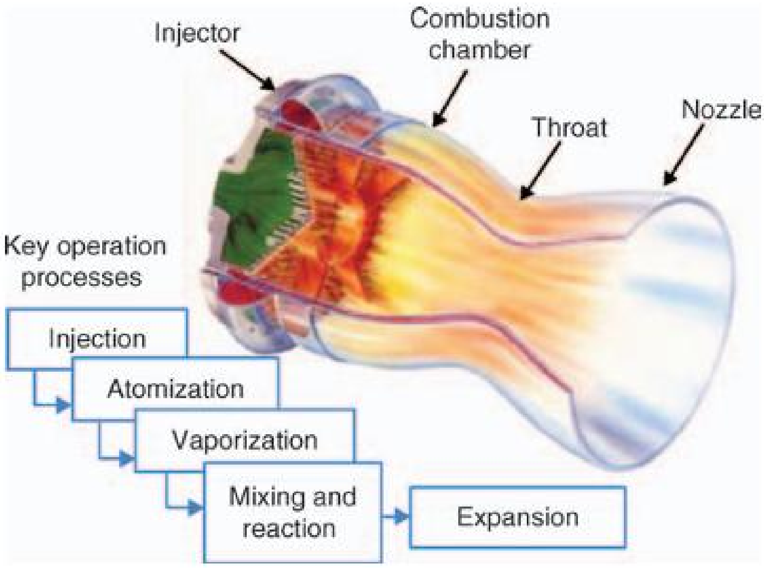

Figure 2.11 Thrust Chamber with integral nozzle and key operation processes (courtesy of Pratt & Whitney Thrusterdyne.)

2.6.1 Injectors

The injector is the part of a thruster engine in which the liquid fuel and liquid oxidizer are admitted into the combustion chamber, broken into particles or droplets to increase the contact surface areas, mixed, and vaporized before reacting in the combustion process. The injector terminates with a perforated plate marking the start of the combustion chamber.

2.6.1.1 Types of Injectors

Several types of injectors have been devised for thruster engines. They can be broadly divided into two categories: (1) nonimpinging and (2) impinging. Among nonimpinging types of injectors, three types, namely, (a) shower head injector, (b) coaxial injector, and (c) swirl atomizers, are used in liquid-propellant thruster engines. The impinging injectors are broadly classified into two: (a) unlike-impinging and (b) like-impinging injectors. All these injectors are discussed in detail in the following.

1. Nonimpinging Injectors:

a. Shower-head Injector: This type of non-impinging injector is one of the earliest designs, in which fuel and oxidizer are ejected perpendicularly from the injector face, resembling the flow from a water shower (see Figure 2.12a(A)). The axial streams of fuel and oxidizer create spray cones or sheets, which interact to promote atomization and mixing through turbulence and diffusion. However, this design tends to produce inefficient atomization and incomplete mixing, necessitating a longer combustion chamber for complete combustion. Despite these drawbacks, the shower-head injector is effective in cooling the combustion chamber walls, as the axial flow helps prevent heat transfer from the combustion zone to the walls. Additionally, it allows for easy throttling of the engine by adjusting the spray cone or sheet width using axially movable sleeves, without causing significant injection pressure drops. This concept was successfully used in the lunar excursion module, demonstrating throttling capabilities with a flow rate range of over 10:1 without substantially altering the mixture ratio.

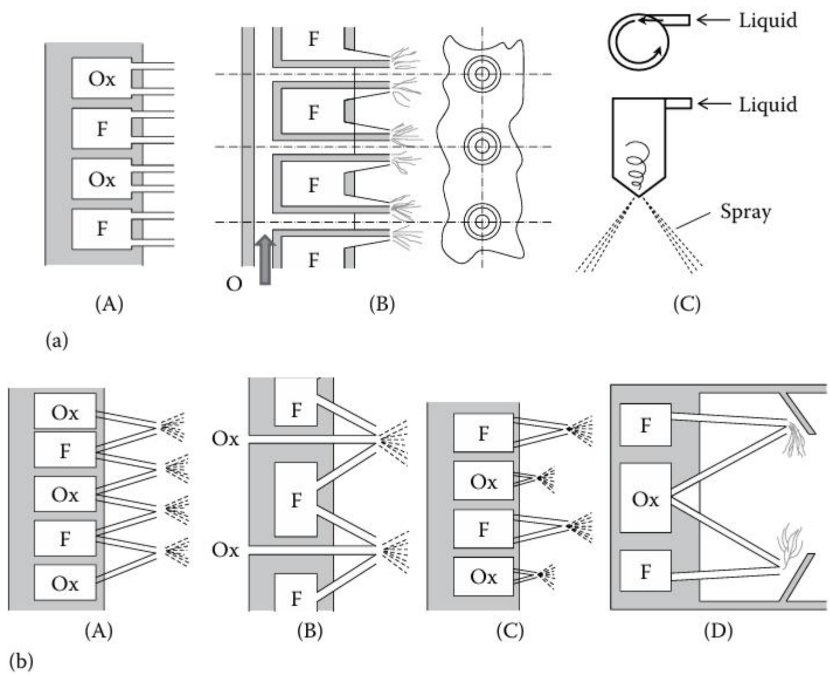

Figure 2.12 Types of injector elements: (a) nonimpinging: (A) shower head, (B) co-axial injector, (C) swirl injector and (b) impinging: (A) unlike doublet, (B) unlike triplet, (C) like doublet, (D) splash plate (Ox, oxidizer; F, Fuel).

b. **Coaxial Injector:** This is the most commonly used non-impinging injector, particularly suitable for non-hypergolic propellants and preferred in semicryogenic liquid-propellant thruster engines. It was first developed by NASA during the early experiments with cryogenic liquid-propellant engines. A typical coaxial injector, as shown in Figure 2.12a(B), consists of two concentric tubes with a recessed length. Generally, the liquid propellant (often liquid oxygen) is injected through the central tube at a relatively low velocity (below 30 m/s), while the gaseous fuel flows through the outer tube at a much higher velocity (over 300 m/s). The slower velocity of the liquid propellant allows for reduced injection speed into the recess area, while the high-velocity gaseous fuel shears the liquid surface into ligaments and then fine droplets, promoting better atomization and mixing. This results in a high-performance, stable injector, which is widely used in semicryogenic thruster engines that utilize gaseous fuel and liquid oxygen. The fuel surrounding the oxidizer helps prevent combustion instability and shields the combustion zone, reducing heat transfer to the combustion chamber walls. However, the performance of the coaxial injector declines significantly when used with two liquid streams, as it becomes difficult to achieve the optimal momentum flux ratio necessary for effective atomization.

c. **Swirl Injector:** In a swirl injector, the liquid propellant is injected tangentially into the injector chamber, causing the formation of a hollow conical sheet with a cone angle ranging from 40° to 100°, as shown in Figure 2.12a(C). This liquid sheet breaks into ligaments and eventually into fine droplets. As the swirl component increases, the cone angle becomes larger, resulting in a more uniform distribution of the droplets. This type of injector is commonly used for non-hypergolic bipropellants that require rapid vaporization and thorough mixing of fuel and oxidizer in the gas phase for efficient combustion. The swirling motion promotes enhanced atomization and facilitates the mixing needed for successful ignition and combustion.

2. Impinging Injectors

In impinging injectors, two or more streams of propellant jets collide with each other, causing the bulk liquid jet or sheet to break up into a fine spray. These injectors are widely used in thruster engines due to their superior performance, simplicity, and lower cost. While impinging injectors are generally preferred for non-hypergolic propellants, they have also been successfully used with hypergolic propellants.

Impinging injectors are categorized into two main types: (1) unlike-impinging injectors, where different propellant streams (fuel and oxidizer) impinge, and (2) like-impinging injectors, where streams of the same propellant impinge.

a. **Unlike-impinging injector:** In this case, two/three different liquid streams impinge on each other when they are issued from two/three angled orifices. Several types of unlike-impinging injectors have been developed for thruster engine applications. Some of them are (a) unlike-impinging doublets, (b) unlike-impinging triplets, which are discussed here:

- **Unlike-Impinging Doublets:** In an unlike-impinging doublet injector, two streams of fuel and oxidizer collide, creating a fan-shaped spray of the mixed liquids, as depicted in Figure 2.12b(A). The impact at the impinging point generates waves that convert the bulk liquid jet or sheet into ligaments, which then fragment into smaller droplets, enhancing atomization and the distribution of fuel and oxidizer in the combustion chamber. The disintegration of the jets results in spherical waves that propagate outward, influencing the extent of the atomization process. Key parameters affecting this process include jet diameter, momentum, injection pressure drop, chamber pressure, and the angle of impingement. When the streams are different, they form a two-dimensional fan-shaped spray in a plane, assuming no chemical reactions occur in the liquid phase. However, various factors, such as momentum mismatches and stream-diameter discrepancies, can distort the spray shape and size, leading to poor atomization and mixing. In hypergolic propellants, rapid chemical reactions can occur simultaneously with atomization, causing reactive-stream separation and affecting performance. Hypergolic propellants have short ignition delays, producing gases before the complete hydrodynamic impact, which can separate the reacting surfaces. Similar effects may occur in non-hypergolic systems, like liquid kerosene and liquid oxygen, particularly under high pressure. Additionally, combustion during the atomization of hypergolic propellants can alter the mixing and mass distribution of the injected spray. The presence of hot gas cross-flow and increased turbulence near the injector can lead to radial winds that deform the spray pattern, stripping away the rapidly atomizing portions of the injected propellants.

- **Unlike-Impinging Triplets:** Unlike-impinging triplet injectors address the issue of distorted spray fans that can occur in doublet injectors due to mismatches in stream size and momentum between fuel and oxidizer streams. This distortion can lead to poor atomization and mixing. In a triplet injector, a symmetrical axial central stream of one propellant is surrounded by two symmetrical impinging streams of another propellant, as shown in Figure 2.12b(B). The triplet configuration can consist of two fuel streams impinging on a single oxidizer stream (F-Ox-F) or two oxidizer streams impinging on a single fuel stream (Ox-F-Ox). The latter configuration is often preferred, as it provides a larger oxidizer area, which is beneficial for mixing, especially in fuel-lean conditions. However, care must be taken to avoid oxidizer-rich streaks near the combustion wall. The primary advantage of the unlike triplet injector is its enhanced mixing capabilities, resulting in higher combustion efficiency compared to doublet injectors. However, it is also more susceptible to combustion instability issues. Various combinations of unlike streams can be utilized to produce the spray, but this increases complexity. Although designs involving quadlets, pentads, or hexads can yield improved mixing, they often result in poorer mass distribution and are rarely used in practice due to their tendency toward instability. Despite these challenges, multiple-impinging injectors with a higher number of streams are advantageous in applications requiring high propellant flow rates.

b. Like-impinging injectors: In this case, two/three or more same liq uid streams are impinged on each other when they are issued from their respective angled orifices. This kind of injectors is also known as self-impinging injectors. Several types of like-impinging injectors have been developed for thruster engine applications. Some of them, namely, (a) like-impinging doublet and (b) like-impinging triplets, are in the following:

- **Like-Impinging Doublets:** In a like-impinging doublet injector, two streams of the same propellant collide, forming a fan-shaped spray of droplets, as shown in Figure 2.12b(C). The impact generates waves along the spray fan's two-dimensional surface, dissipating energy and converting the bulk liquid jet into ligaments that fragment into smaller droplets. Unlike unlike-impinging doublets, there is no mixing between the streams since they consist of the same liquid. The degree of mixing is influenced by the orientation of the initial fans for secondary impingements and the overlapping of sprays. Like-impinging injectors are typically used in thruster engines with non-hypergolic liquid propellants, as they mitigate the reactive demixing issues seen in unlike-impinging injectors, ensuring higher combustion stability. While they provide lower mixing levels than unlike-impinging doublets, effective design improvements can enhance combustion efficiency

- **Like-Impinging Triplets:** To overcome the issue of undesired shifts in the impinging point caused by mismatches in stream size and momentum, like-impinging triplet injectors allow three identical propellant streams to collide at a single point, as illustrated in Figure 2.12. These triplets typically produce a narrower spray fan with larger droplets compared to doublet injectors, which may result in overall performance losses. Additionally, smaller orifices are required to accommodate more triplet injectors within the same manifold surface area. Similar challenges can arise with other multiple-stream self-impinging injectors, such as quadlets and pentads, potentially complicating design and performance.

3. Other Types of Injectors

Several other types of injectors have been tried during the development of thruster engines. Two of them, namely, (1) splash plate and (2) premixing injectors, shown in Figure 2.12, are discussed:

a. Splash Plate Injector: The splash plate injector utilizes the principle of impingement in conjunction with a splash plate, as shown in Figure 2.12b(D). This design promotes the breaking of liquid jets or sheets, facilitating better mixing of the propellants in their liquid state. By directing the liquid streams against the splash plate, the injector minimizes the misalignment issues associated with the impinging points seen in doublet configurations. This feature enhances performance across a wide range of operating conditions and has been successfully applied to certain storable propellants.

b. Premixing Injector: In a premixing injector, the liquid fuel and oxidizer are mixed prior to being injected into the combustion chamber. The dimensions of the premixing chamber are influenced by the reaction time and the residence time of the propellant streams. It is crucial to avoid explosions of the premixed propellants within the chamber, particularly because flame can travel back from the combustion chamber, leading to dangerous conditions—especially under high-pressure and high-mass-flux scenarios. To mitigate this risk, swirls may be introduced into the liquid stream. Due to these safety concerns, premixing injectors are uncommon in thruster engines, although they can be used in the combustion chambers of other types of engines. While they have been tested with non-hypergolic propellants, they can cause excessive thermal loads on the injector structure due to potential precombustion in the premixing chamber. Consequently, the use of premixing injectors is typically reserved for addressing specific injection challenges.

2.6.2 Combustion Chambers

A liquid-thruster combustion chamber is designed to convert propellants into high-temperature, high-pressure gas through combustion, releasing the chemical energy of the propellant and increasing the internal energy of the gas. Traditionally, combustion chambers have been of tubular construction and are a critical part of the thrust chamber, where nearly all of the propellant burning takes place. The chamber serves as an envelope to retain the propellants long enough to ensure complete mixing and combustion, referred to as the "stay time."

Historically, three geometric shapes have been used in combustion chamber design: spherical, near-spherical, and cylindrical.Three geometrical shapes that have been used in combustion-chamber design are shown in Figure 2.13. A spherical combustion chamber has, in comparison with a cylindrical one of the same volume, a smaller mass and a smaller surface to be cooled. In addition, for the same pressure and for the same strength of the materials used, the walls of a spherical combustion chamber can be less thick than those of a cylindrical combustion chamber. On the other hand, a spherical combustion chamber is more difficult to manufacture and offers a lower performance than is the case with a cylindrical combustion chamber. However, despite these advantages, spherical chambers are more difficult to manufacture and generally provide poorer performance in other respects, leading to the more frequent use of cylindrical chambers.

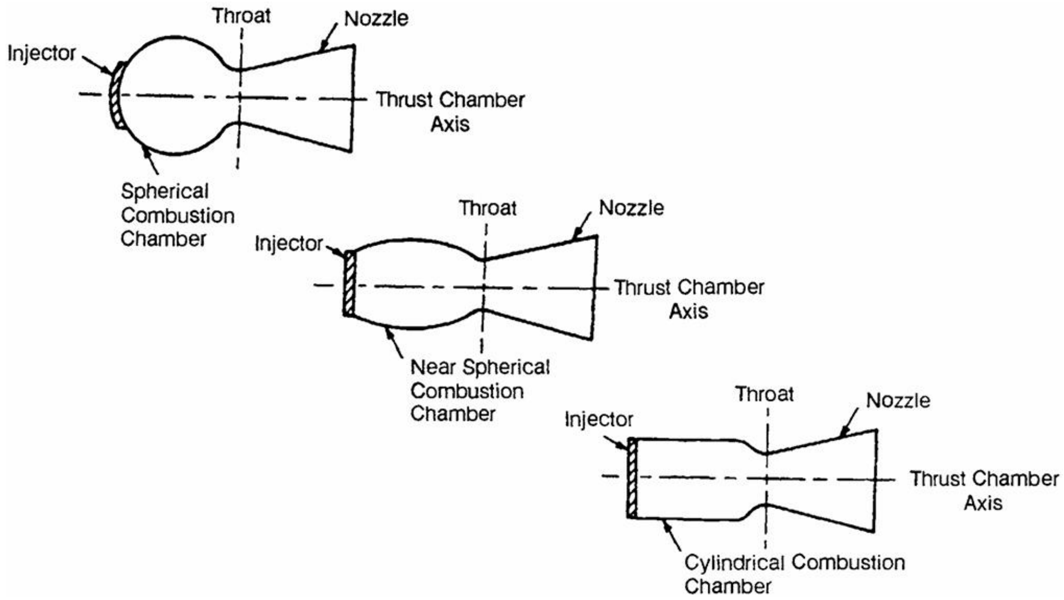

Figure 2.13 Frequently used geometrical shapes for combustion chambers.

2.6.3 Nozzles

The primary function of a thruster nozzle is to efficiently convert the thermal energy of combustion gases into kinetic energy, producing high exhaust velocities. Typically, thruster nozzles are converging-diverging (De Laval) designs, where gas is accelerated to sonic speed at the throat and to supersonic speed in the diverging section. The nozzle increases thrust by converting high-pressure, high-temperature gases into velocity.

Maximum thrust is achieved when the exhaust gas pressure at the nozzle exit matches the ambient pressure, a condition called optimum nozzle expansion.

When the exit pressure differs from the ambient pressure, two scenarios occur:

- **Over-expansion** (exit pressure less than ambient), leading to shocks and pressure adjustments through repeating compression and expansion waves (Mach disks).
- **Under-expansion** (exit pressure greater than ambient), where the flow expands and compresses in a series of Prandtl-Meyer expansions and compressions to reach pressure equilibrium.

2.6.3.1 Nozzle Shape

Most thruster nozzles are of the converging-diverging De Laval design. In the converging section, where gas flow velocity is relatively low, a smooth and well-rounded contour results in minimal energy losses. However, the diverging section's shape is critical due to the high flow velocities involved. The optimal nozzle shape for a specific expansion area ratio is guided by key design goals:

- Ensuring uniform, parallel, and axial gas flow at the exit for maximum momentum.
- Minimizing flow separation and turbulence losses.
- Keeping the nozzle as short as possible to reduce weight, space, friction losses, and cooling needs.
- Facilitating ease of manufacturing.

To avoid shock waves or turbulence, abrupt changes in the nozzle wall contour should be avoided. While the nozzle throat represents the minimum cross-sectional area, it is typically designed with a smooth, rounded contour. Only the nozzle exit features a sharp edge to prevent over-expansion and flow separation.

Various nozzle shapes have been studied, tested, and used in liquid thruster engines. The most common types include conical, contoured, plug (aerospike), and expansion-deflection nozzles and are shown in Figure1-14(a to d).

a. Conical nozzle:

Conical nozzles are simple to design and manufacture with flexibility in resizing. Thus, the conical nozzle was widely used in early experimental liquid thruster engines. This simple geometry, however, comes with the penalty of decreased performance due to the radial component of the exhaust gas velocity. Optimum-divergence cone half angles are generally between 12◦ and 18◦ as shown in Figure1-14a in terms of performance and nozzle size. Small divergence angles result in low divergence losses, but increase the noz zle length and weight. In contrast, large divergence angles increase the divergence losses, but result in lower length and weight.

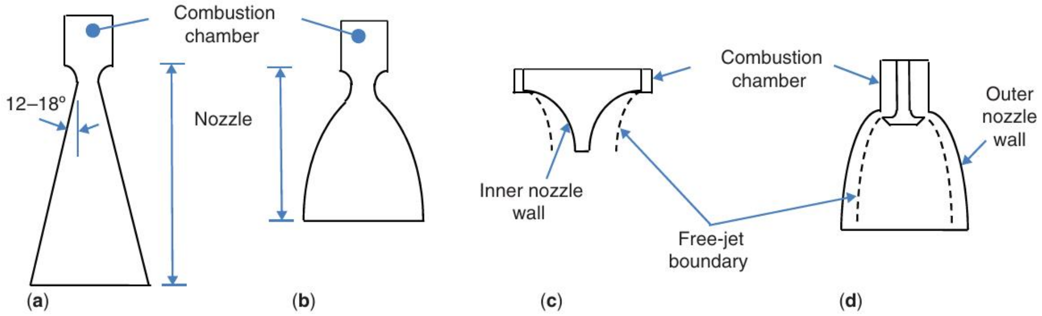

Figure 2.14 Most common nozzle shapes: (a) conical; (b) contoured; (c) plug; (d) expansion–deflection.

b. Contoured Nozzle:

Contoured nozzles offer superior performance and reduced length compared to conical nozzles, making them the preferred choice in modern liquid thruster engines. The most common configuration is the bell-shaped nozzle as shown in Figure 2.14b, which features an initial section with a high expansion angle (30°–60°) immediately after the throat. This is followed by a gradual reduction in the contour slope, resulting in a near-zero divergence angle at the nozzle exit.

The large divergence angles near the throat are made possible by the rapid acceleration of flow, which prevents flow separation when the nozzle contour is smooth. The sudden expansion behind the throat generates weak expansion waves, while the reversal of the contour slope creates compression waves as the flow is redirected. The expansion waves from the throat region counteract the compression effects, minimizing nozzle losses.

A nearly uniform distribution of exit velocity can be achieved with minimal divergence loss, but the length of an ideal bell-shaped nozzle is typically too long. Proper contour shaping, however, can reduce the nozzle length by 10–25% compared to a 15° conical nozzle. Bell-shaped nozzles are usually designed using Rao's parabolic approximation, derived from the method of characteristics.

Similar to thrust chamber design, the nozzle can be cooled using various techniques: (i) regenerative cooling, (ii) film cooling, (iii) transpiration cooling, (iv) ablative cooling, and (v) radiative cooling. The choice of cooling method depends on careful consideration of design trade-offs.

- **Parabolic approximation of the bell nozzle:**

The parabolic approximation, proposed by G. V. R. Rao, is a convenient method for designing near-optimum-thrust bell nozzles. The design configuration of a parabolic approximation bell nozzle is shown in Figure 2.15. In this design, the nozzle contour just upstream of the throat is a circular arc with a radius of 1.5 times the throat radius Rt. The divergent section consists of a circular entrance section with a radius of 0.382 Rt from the throat to point N, and a parabolic contour from N to the exit. The design process requires key data, such as the throat diameter, nozzle length, expansion area ratio, and the initial and exit wall angles. By selecting appropriate inputs, an optimal nozzle contour can be approximated accurately, with minimal influence from the specific heat ratio of the propellant.

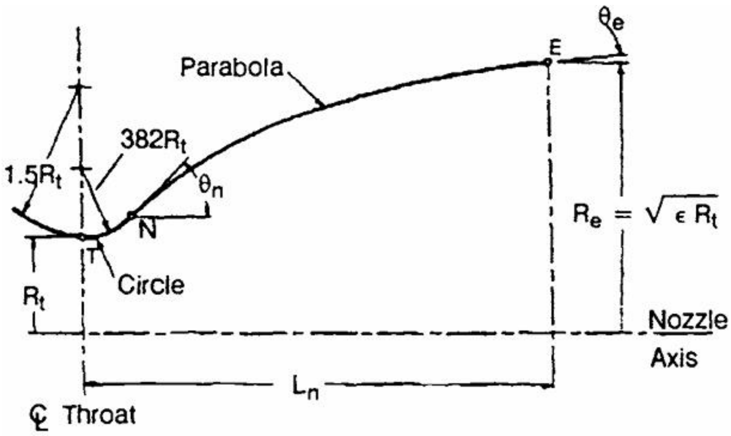

Figure 2.15 Parabolic approximation of bell nozzle.

c. Annular nozzles (plug and expansion–deflection) :

Comparedtoaconicalorbell-shapednozzle,annularnozzles are more complex to design and operate. There are two basic types of annular nozzles: (i) plug (or commonly known as aerospike) nozzle and (ii) expansion–deflection nozzle. As shown in Figure 2.14c, the plug nozzle has the outer surface of the annular flowasafree-jet boundary, whichisself-adjusted by ambient pressure. Similarly, the expansion–deflection nozzle has the inner free-jet boundary with the outer nozzle wall contour as shown in Figure 2.14d. Because of the altitude compensation characteristics with the free-jet boundary, annular nozzles are not subject to flow separation losses from over-expansion at low altitude as in the case of a conventional nozzle. Also, it allows a short nozzle design, potentially reducing interstage structural weight. However, annular nozzles require relatively high cooling require ments, heavier structural construction, and manufacturing complexity.

2.7 Computer-Aided Engineering (CAE) Tools

In designing and optimizing the LOX/LCH4 thruster engine, various Computer-Aided Engineering (CAE) tools are employed to model, simulate, and analyze key aspects of the engine’s performance. These tools provide essential insights into combustion processes, thermal management, and fluid dynamics, allowing for effective design validation and optimization. This section highlights the main CAE tools used in the project.

2.7.1 Rocket Propulsion Analysis (RPA[1])

RP Software+Engineering UG offers Rocket Propulsion Analysis (RPA), a powerful software tool used for preliminary analysis and design of liquid Thruster engines. RPA is widely used in the industry due to its ability to calculate engine performance based on input parameters such as propellant type, chamber pressure, and mixture ratio. Key features of RPA include:

- **Thrust and Specific Impulse Calculation:** RPA provides detailed calculations of thrust, specific impulse (Isp), and propellant flow rates for various engine configurations.
- **Performance Optimization:** The software allows for optimization of key parameters such as expansion ratio and chamber pressure to achieve the desired performance levels.
- **Combustion Analysis:** RPA can simulate combustion conditions, predicting temperature, pressure, and gas composition in the combustion chamber and nozzle.

RPA serves as an essential tool for the initial design phase, providing a solid foundation for more detailed simulations using other CAE tools.

2.7.2 NASA CEA

CEA (Chemical Equilibrium with Applications) is a NASA software tool used to calculate the thermodynamic properties of combustion products and predict chemical equilibrium for a wide range of Thruster engine conditions. Key capabilities of CEA include:

[1] See https://rocket-propulsion.com/index.htm

Equilibrium Calculations: CEA calculates the composition, temperature, and pressure of combustion gases at equilibrium, providing valuable data for understanding the behavior of the propellants under different operating conditions.

Performance Estimation: The software is used to estimate important engine parameters such as specific impulse, thrust, and exhaust velocity based on the propellant chemistry and engine design.

Propellant Mixture Ratio Optimization: CEA helps optimize the LOX/LCH4 mixture ratio for maximum combustion efficiency and performance.

CEA NASA is particularly useful for validating combustion models and ensuring that the chemical reactions inside the engine are correctly represented.

The combination of RPA and CEA NASA provides a comprehensive toolkit for the design, simulation, and optimization of the LOX/LCH4 thruster engine. These tools allow for accurate performance predictions, detailed combustion analysis, and efficient design optimization, ensuring the engine meets all mission requirements while operating efficiently and reliably.

3 Thruster Calculation

3.1 Calculation of Stoichiometric Mixture Ratio for LOX/LCH_4

To determine the stoichiometric mixture ratio for the propellant combination of liquid oxygen (LOX) and liquid methane (LCH_4), the following steps are followed:

- **Step 1: Balanced Chemical Equation**

The combustion reaction for liquid methane with liquid oxygen can be expressed as:

$$\text{CH4 + O2} \rightarrow \text{CO2 + H2O} \tag{3-1}$$

- **Step 2: Balancing the Equation**

The balanced chemical equation for the combustion of methane is:

$$\text{CH4 + 2O2} \rightarrow \text{CO2 + 2H2O} \tag{3-2}$$

From this equation, it is evident that one mole of methane (CH4) reacts with two moles of oxygen (O2).

- **Step 3: Molar Mass Calculations**

The molar masses of the reactants are calculated as follows:

➢ **Molar mass of CH4 (methane):**

Carbon (C): 12.01 g/mol

Hydrogen (H): 1.008 g/mol×4=4.032 g/mol

Total: 12.01+4.032=16.042 g/mol

➢ **Molar mass of O2 (oxygen):**

Oxygen (O): 16.00 g/mol×2=32.00 g/mol

- **Step 4: Calculating the Stoichiometric Mixture Ratio**

The stoichiometric mixture ratio (O/F) can be determined using the formula:

$$\mathrm{O/F} = \frac{moles\ of\ O_2}{moles\ of\ CH_4} \tag{3-3}$$

From the balanced equation, we find:

$$\mathrm{O/F} = \frac{2\ moles\ of\ O_2}{1\ moles\ of\ CH_4} = 2 \tag{3-4}$$

- **Step 5: Mass Ratio Calculation**

To calculate the mass ratio, the following equation is used:

$$\text{Mass Ratio (O/F)} = \text{MR} = \frac{\text{Mass of O}_2}{\text{Mass of CH}_4} = \frac{2 \times 32.00\ \text{g/mol}}{16.042\ \text{g/mol}} = \frac{64.00}{16.042} \approx 4 \tag{3-5}$$

This indicates that the stoichiometric mixture ratio by mass of LOX to LCH_4 is approximately 4. Thus, for every 1 kg of methane, about 4 kg of liquid oxygen is required for complete combustion.

- **Step 6: Adjusting for Practical Applications**

While the calculated value of 4 serves as a theoretical baseline, it is typically adjusted for practical applications, where the commonly cited stoichiometric mixture ratio falls around 3.2 to 3.5. This adjustment accounts for various factors such as:

Real-World Engine Efficiencies: Actual Thruster engines may not achieve perfect stoichiometric ratios due to design limitations or optimization for performance.

Combustion Characteristics: The combustion behavior can differ based on mixture preparation, injector design, and combustion chamber conditions.

Hydrogen Addition: In some designs, a small amount of hydrogen may be introduced to enhance combustion, effectively reducing the oxygen requirements.

3.2 Optimal Mixture Ratio Analysis

As previously discussed, the optimal mixture ratio for the LOX/LCH_4 propellant system may differ from the stoichiometric ratio, depending on performance and thermal constraints. This section utilizes NASA CEA calculations to determine the most efficient operational parameters for the engine by identifying the mixture ratio that maximizes specific impulse (Isp) while considering chamber temperature limits.

3.2.1 Parameters for the Analysis

NASA CEA will be used to conduct simulations for each mixture ratio within the specified parameters. The inputs for each simulation will include:

- **Fuel:** Liquid Methane (LCH_4)
- **Oxidizer:** Liquid Oxygen (LOX)
- **Chamber Pressure (Pc):** The simulations will be conducted at a chamber pressure of 300 psia, which represents typical operational conditions for many Thruster engines.
- **Chamber to exit pressure ratio:** The chamber-to-exit pressure ratio (Pc/Pe) will be set to 30,000,000,000 to simulate vacuum conditions, where the external pressure is nearly zero. In practical terms, we approximate the exit pressure Pe as 10^{-8} psia to reflect the near-vacuum environment of space.
- **Mixture Ratios:** The analysis will explore O/F mass ratios ranging from 2.0 to 4.6, with increments of 0.04. This range enables a comprehensive examination of how different LOX-to-LCH_4 proportions influence specific impulse and chamber temperature.
- **Area Ratio (A_e/A_t):** To ensure a feasible thruster design, the area ratio was limited to a maximum of 100, as the optimal area ratio from initial calculations was impractically large for a vacuum environment. By setting A_e/A_t = 100, the design is adjusted to more realistic dimensions, balancing theoretical efficiency with manufacturable limits.

The simulations will yield specific impulse (Isp) and chamber temperature values for each mixture ratio, allowing for the identification of the optimal fuel and oxidizer proportion to maximize efficiency.

3.2.2 Analysis Based on Specific Impulse and Chamber Temperature

To identify the optimal mixture ratio for the LOX/LCH_4 propulsion system, both the specific impulse (Isp) and the chamber temperature as functions of the oxidizer-to-fuel (O/F) mass ratio were analyzed. The goal was to find a balance between maximizing performance (high Isp) and maintaining manageable thermal conditions (chamber temperature) to enhance engine durability and efficiency. The graphs below illustrate these variations.

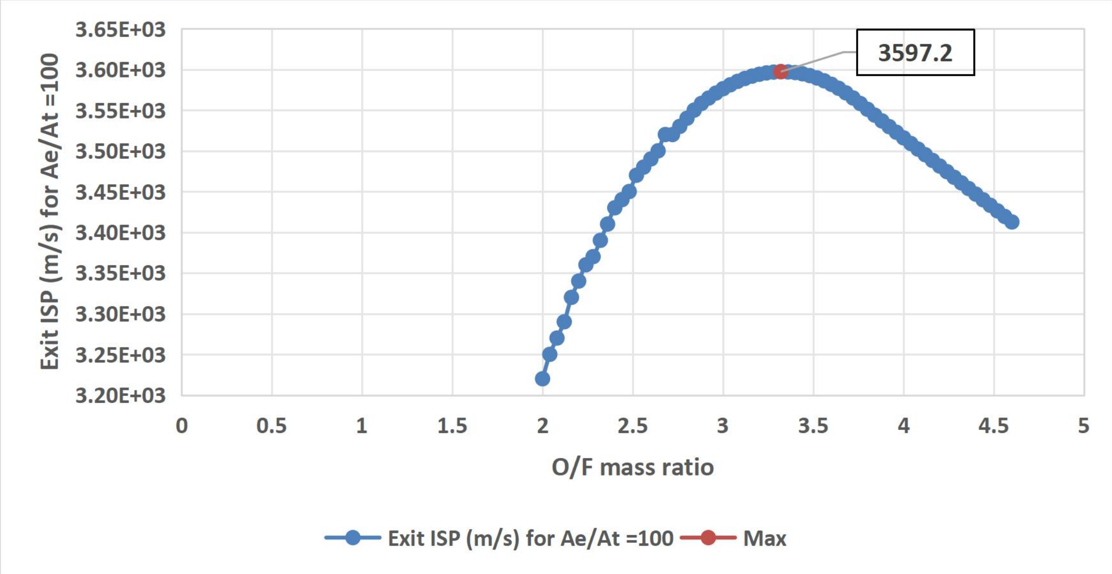

Figure 3.1 Specific Impulse (Isp) vs. O/F Mass Ratio at 300 psia Chamber Pressure in Vacuum Conditions (NASA CEA Results)

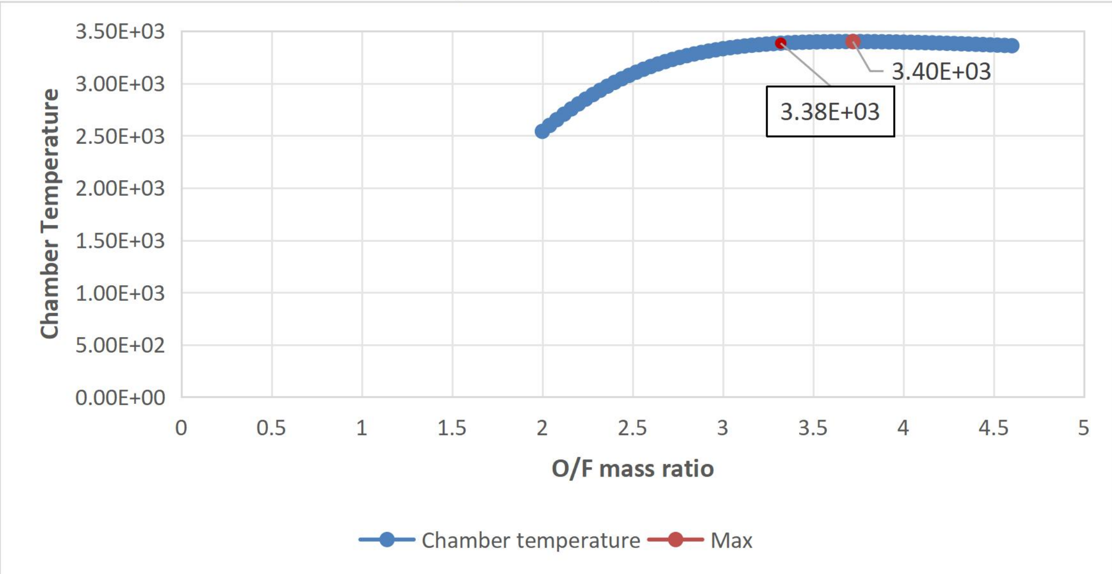

Figure 3.2 Chamber Temperature vs. O/F Mass Ratio at 300 psia Chamber Pressure in Vacuum Conditions (NASA CEA Results)

3.2.2.1 Specific Impulse and Chamber Temperature Comparison

The specific impulse curve, as shown in Figure 6.1, peaks at an O/F ratio of approximately 3.32, where the exit Isp reaches around 3597.2 m/s. This mixture ratio offers the highest efficiency in terms of thrust production for the LOX/LCH_4 system, making it an attractive option from a performance standpoint.

In contrast, Figure 6.2 reveals that the chamber temperature continues to rise with the O/F ratio, reaching a maximum at an O/F ratio of around 3.72, where the temperature is approximately 3400 K. However, at the O/F ratio that maximizes specific impulse (3.32), the chamber temperature is slightly lower than this peak, around 3380 K.

3.2.2.2 Determining the Optimal Mixture Ratio

This discrepancy between the O/F ratios for maximum Isp and maximum chamber temperature highlights an important trade-off. Operating at the O/F ratio of 3.32 achieves the highest specific impulse, thereby maximizing thrust efficiency. However, the chamber temperature at this ratio is still very close to the maximum observed temperature, which could impose significant thermal stress on the combustion chamber and require advanced cooling solutions.

The optimal mixture ratio for the LOX/LCH_4 system is identified as 3.32, where specific impulse is maximized, and the chamber temperature remains near, but not at, the peak level. This selection provides a balance between maximizing performance and maintaining thermal conditions that support engine durability.

3.3 Performance Parameters of the Thruster at Optimal Mixture Ratio Analysis

In this section, we analyze key performance parameters for the LOX/LCH_4 propulsion system at the optimal mixture ratio of 3.32, as determined in Section 3.2. Using NASA CEA data, we explore the performance characteristics across three main regions of the rocket nozzle: the chamber, throat, and exit. This analysis includes values for specific impulse, thrust coefficient, and other thermodynamic properties critical to understanding the engine's efficiency and thermal management requirements.

3.3.1 Definitions of NASA CEA Output Parameters

- **Thrust Coefficient (Cf):** A dimensionless parameter that measures the efficiency of a rocket nozzle, defined as the thrust produced per unit pressure in the combustion chamber.
- **Mach Number:** A dimensionless quantity representing the ratio of the speed of the flow to the speed of sound in that medium, indicating whether the flow is subsonic, sonic, or supersonic.
- **Gamma (γ):** The specific heat ratio of the gas, defined as the ratio of specific heat at constant pressure (Cp) to specific heat at constant volume (Cv), influencing the thermodynamic behavior of the flow.
- **Cross-section Area Ratio (Ae/At):** The ratio of the exit area (Ae) of the nozzle to the throat area (At), used to evaluate the expansion and acceleration of the exhaust gases through the nozzle.
- **Pressure (P):** The static pressure of the gas at various points in the propulsion system, measured in bar, indicating the energy available for propulsion.
- **Sonic Velocity (a):** The speed at which pressure waves travel through the gas, dependent on the gas properties and temperature, critical for determining flow characteristics in the nozzle.
- **Density (ρ):** The mass per unit volume of the gas, measured in kg/m^3, affecting both the mass flow rate and the thrust generated by the engine.
- **Enthalpy (h):** The total heat content of the gas, measured in J/kg, representing the energy available for doing work during expansion.

- **Entropy (s):** A measure of the disorder or randomness of the gas, expressed in J/(kg·K), indicating the irreversibility of processes and the energy unavailable for work.
- **Gibbs Energy (G):** The energy associated with a system that can perform work at constant temperature and pressure, measured in J/kg, useful for evaluating the feasibility of chemical reactions.
- **Internal Energy (u):** The total energy contained within the gas due to its temperature and state, expressed in J/kg, influencing the thermodynamic efficiency of the engine.
- **Molecular Weight (M):** The mass of a molecule of gas, expressed in g/mol, affecting the gas properties and performance of the propulsion system.
- **Temperature (T):** The absolute temperature of the gas in Kelvin (K), which influences the thermodynamic properties and performance characteristics of the engine.

3.3.2 Performance Parameters from NASA CEA

The data obtained from the NASA CEA simulations provide critical insights into the performance parameters for each station (Chamber, Throat, Exit and Exit at Ae/At = 100) of the LOX/LCH_4 propulsion system at the optimal mixture ratio of 3.32. The results are summarized in Tables 3.1.a, 3.1.b and 3.1.c.

Station	Thrust Coefficient (Cf)	Mach Number	Gamma (γ)	(Ae/At)	Pressure (P, bar)
Chamber	0.0000E+00	0.0000E+00	1.1258E+00	0.0000E+00	2.0684E+01
Throat	6.5121E-01	1.0000E+00	1.1228E+00	1.0000E+00	1.1997E+01
Exit	2.3933E+00	1.7621E+01	1.0000E+00	2.3123E+08	6.8947E-10
Exit at Ae/At = 100	1.9740E+00	4.5072E+00	1.2059E+00	1.0000E+02	1.6667E-02

a

Station	Sonic Velocity (m/s)	Specific Heat (Cp, kJ/(kg·K))	Specific Impulse (Isp, m/s))	Density (ρ) (kg/m³)	Enthalpy (h) (J/kg)
Chamber	1.2246E+03	8.2199E+00	0.0000E+00	1.5527E+00	-1.5993E+03
Throat	1.1867E+03	7.9788E+00	1.1867E+03	9.5647E-01	-2.3034E+03
Exit	2.4750E+02	1.2656E+06	4.3613E+03	1.1255E-09	-1.1110E+04
Exit at Ae/At = 100	7.9809E+02	2.1095E+00	3.5972E+03	3.1554E-03	-8.0691E+03

b

Station	Entropy (s) (J/(kg·K))	Gibbs Energy (G) (J/kg)	Internal Energy(u) (J/kg)	Molecular Wt. (M) (mw) (g/mol)	Temperature (t) (K)	Pc/Pe
Chamber	1.2733E+01	-4.4689E+04	-2.9314E+03	2.1121E+01	3.3840E+03	1.0000E+00
Throat	1.2733E+01	-4.3437E+04	-3.5577E+03	2.1414E+01	3.2304E+03	1.7241E+00
Exit	1.2733E+01	-1.3550E+04	-1.1171E+04	2.3120E+01	1.9164E+02	3.0000E+10
Exit at Ae/At = 100	1.2733E+01	-2.6756E+04	-8.5973E+03	2.3101E+01	1.4676E+03	1.2410E+03

c

Table 3.1 performance parameters for each station (Chamber, Throat, Exit and Exit at Ae/At = 100) at the optimal mixture ratio (NASA CEA Results)

3.3.3 Interpretation of NASA CEA Results

The NASA CEA results provide detailed insights into the performance parameters and thermodynamic properties of the LOX/LCH_4 thruster engine at various critical points: the chamber, throat, and exit, along with an additional exit condition using a limited area ratio (Ae/At = 100). These parameters are crucial for assessing the engine's efficiency, thermal behavior, and feasibility of design in vacuum conditions. The following is an interpretation of key findings based on these results:

3.3.3.1 Operating Conditions and Inputs:

- The chamber pressure is set to 300 psia with an extremely high chamber-to-exit pressure ratio of 3×10^{10}, simulating an ideal vacuum.
- An oxidizer-to-fuel ratio (O/F) of 3.32 is used, close to the specific impulse peak, optimizing performance.
- The analysis considers liquid methane (CH_4) as the fuel and liquid oxygen (O_2) as the oxidizer, with full combustion assumed.

3.3.3.2 Performance Parameters:

- **Thrust Coefficient (Cf):** The thrust coefficient shows a significant increase from the throat to the exit, with a maximum value of 2.3933 at the exit. This indicates the high efficiency of the nozzle in converting combustion energy into thrust. However, at an area ratio of 100, the exit thrust coefficient drops slightly to 1.9740. This more practical area ratio still allows for efficient thrust production while maintaining structural feasibility.
- **Effective Exhaust Velocity (c):** Effective exhaust velocity is the speed at which exhaust gases effectively exit the nozzle, considering both the exit velocity v_e and pressure differential at the exit Ae(pe−pa).

$$c = V_e + A_e(P_e - P_a) \tag{3-6}$$

In vacuum conditions where pe=pa=0, c=v_e. for this engine, the effective exhaust velocity c at the vacuum exit is 4361.3 m/s, representing the highest achievable efficiency. With Ae/At limited to 100, c slightly decreases to 3597.2 m/s, providing a more practical value without a severe loss of performance. This compromise between maximum Isp and realistic area ratios helps balance performance with feasible nozzle dimensions.

- **Specific Impulse (I_{sp}):** Specific impulse measures the thrust generated per unit weight flow rate of the propellant, typically in seconds. Since NASA CEA provides c, the specific impulse can be derived by dividing c by gravitational acceleration g≈9.81 m/s2, yielding:

$$\mathrm{Isp} = \frac{\mathrm{c}}{\mathrm{g}} = \frac{3597.2\ \mathrm{m/s}}{9.81\ \mathrm{m/s^2}} = 366.687\ \mathrm{s} \tag{3-7}$$

- **C*, (m/s):** Characteristic velocity, indicating the performance of the engine in terms of combustion efficiency. C* remains constant across all stations at 1822.3 m/s, indicating stable combustion efficiency.

3.3.3.3 Thermodynamic Properties:

- **Temperature (T):** The temperature in the chamber reaches 3384 K, aligning with the high energy release of the combustion process. At the vacuum exit, the temperature falls to 191.64 K, while at Ae/At = 100, the exit temperature is 1467.6 K, a more reasonable temperature for material durability and nozzle design.
- **Density (ρ):** Density decreases from 1.5527 kg/m³ in the chamber to near vacuum levels at the exit, due to gas expansion. For Ae/At = 100, density is 0.00315 kg/m³, indicating a lower but manageable expansion for real-world applications.
- **Sonic Velocity (a):** The sonic velocity decreases from 1224.6 m/s in the chamber to 247.5 m/s at the vacuum exit, reflecting cooling and expansion of the exhaust gases. For Ae/At = 100, the sonic velocity remains high at 798.09 m/s, allowing for a controlled supersonic flow within feasible design limits. It reflects the thermal energy being converted into kinetic energy as the gas expands, accelerating the flow to supersonic speeds downstream of the throat.
- **Specific Heat (Cp):** The specific heat Cp decreases progressively from 8.22 kJ/(kg·K) in the chamber to 7.98 kJ/(kg·K) at the throat and 2.11 kJ/(kg·K) at the exit. This reduction reflects the energy transformation as gases expand and cool. High Cp in the chamber supports efficient energy release during combustion, while the lower Cp at the exit indicates successful energy conversion to achieve high exhaust velocity.
- **The enthalpy** and **internal energy** values provide insight into the energy available for work at each station, with both values dropping significantly as the exhaust gases expand.
- **The entropy** remains constant across stations, suggesting minimal irreversibility in the expansion process, while **Gibbs energy** values reflect the thermodynamic feasibility of reactions at each stage.

3.3.3.4 Flow and Expansion Characteristics:

- **Mach Number:** In the chamber, the Mach number is zero, as expected in subsonic regions. It reaches unity at the throat, marking the transition to supersonic flow, and increases dramatically to 17.621 at the ideal exit, demonstrating high gas acceleration under vacuum conditions. For an area ratio of 100, the exit Mach number is reduced to 4.5072, providing a controlled supersonic expansion that remains manageable for structural and thermal stability.
- **Gamma (γ):** The specific heat ratio (γ) remains relatively stable across stations but decreases slightly at the exit, which indicates changes in gas properties at low pressures. This variation reflects shifts in specific heat capacities during the expansion process.

3.3.3.5 Molecular Properties:

- **Molecular Weight (M):** The molecular weight slightly increases from the chamber to the exit, with values ranging from 21.121 to 23.101 g/mol. This gradual increase reflects changes in gas composition due to varying pressure conditions during expansion.

3.3.3.6 Design Feasibility:

- **Cross-section Area Ratio (Ae/At):** An area ratio of 2.3123×10^{8} is required for ideal vacuum expansion, which is unfeasible in practical applications. Limiting the area ratio to 100 provides significant expansion while keeping the design achievable.
- **Pressure (P):** Pressure decreases dramatically from 20.684 bar in the chamber to nearly zero at the exit under ideal vacuum. With Ae/At = 100, the exit pressure is 0.01667 bar, providing a feasible low-pressure environment for significant expansion without compromising nozzle integrity, facilitating the acceleration of exhaust gases to high velocities.

3.4 Thrust and Mass Flow Calculations

3.4.1 Total Mass Flow Rate:

To determine the total mass flow rate ṁ, we use the relationship between thrust F, effective exhaust velocity c, and total mass flow rate as follows:

$$\dot{m} = \frac{F}{c} \tag{3-8}$$

Given an assumed thrust force of 5 kN and the effective exhaust velocity c derived from NASA CEA as 3597.2 m/s, we obtain ṁ = 1.39 Kg/s

This parameter is critical for determining the specific fuel and oxidizer flow rates required to sustain the desired thrust.

3.4.2 Fuel and Oxidizer Mass Flow Rates:

The mass flow rates for fuel $\dot{m}_{CH4}$ and oxidizer $\dot{m}_{O2}$ are derived based on the mixture ratio O/F MR=3.32. Using the relationships:

$$\dot{m}_{CH_4} = \frac{\dot{m}}{1 + MR} = \frac{1.39}{1 + 3.32} = 0.3217\ \mathrm{Kg/s} \tag{3-9}$$

$$\dot{m}_{O_2} = \frac{\dot{m}}{1 + {}^{1}/_{MR}} = \frac{1.39}{1 + {}^{1}/_{3.32}} = 1.0682 \text{ Kg/s} \tag{3-10}$$

These calculations provide the basis for configuring the propellant feed system, ensuring accurate delivery of both fuel and oxidizer to meet thrust requirements while maintaining the optimal mixture ratio.

3.5 Nozzle Geometry Calculations

3.5.1 Throat Area and Diameter

The throat area At is a key design parameter that supports the nozzle's ability to choke the flow and achieve critical conditions. It is calculated using the equation for characteristic velocity (c*):

$$c^* = \frac{P_c \times A_t}{\dot{m}} \tag{3-11}$$

where c* is provided by NASA CEA, and Pc is the chamber pressure assumed as 300 psia = 2.06843×10^6 Pa.

Rearranging for At:

$$A_t = \frac{\dot{m} \times c^*}{P_c} = \frac{1.39\, Kg/s \times 1822.3\, m/s}{2.06843 \text{ x } 10^6 \text{ Pa}} = 1.2246 \times 10^{-3}\, m^2 \tag{3-12}$$

The throat diameter (Dt) is then:

$$D_t = \sqrt{\frac{4\, A_t}{\pi}} = \sqrt{\frac{4 \times 1.2246 \times 10^{-3}}{\pi}} = 0.039486\, m = 3.9486\, cm \tag{3-13}$$

3.5.2 Exit Area and Diameter

Using the area ratio Ae/At = 100, the exit area Ae can be calculated as follows:

$$A_e = 100 \times A_t = 100 \times 1.2246 \times 10^{-3} = 0.12246\, m^2 \tag{3-14}$$

The exit diameter De is then calculated as:

$$D_e = \sqrt{\frac{4\, A_e}{\pi}} = \sqrt{\frac{4 \times 0.12246}{\pi}} = 0.39486\, m = 39.486\, cm \tag{3-15}$$

3.6 Combustion Chamber Geometry

3.6.1 Combustion Chamber Area and Diameter

Assuming a contraction ratio Ac/At = 4, the combustion chamber area Ac is calculated as:

$$A_c = 4 \times A_t = 4 \times 1.2246 \times 10^{-3} = 4.8983 \times 10^{-3}\, m^2 \tag{3-16}$$

the chamber diameter Dc is then calculated as:

$$D_c = \sqrt{\frac{4\, A_c}{\pi}} = \sqrt{\frac{4 \times 4.8983 \times 10^{-3}}{\pi}} = 0.078973\, m = 7.8973\, cm \tag{3-17}$$

3.6.2 Combustion Chamber Volume

The volume Vc of the combustion chamber is essential for maintaining a stable combustion process. It is calculated using the characteristic length L* and throat area At as:

$$V_C = L^* \times A_t \tag{3-18}$$

The characteristic length, L*, is a design parameter in rocket engine combustion chambers that represents the effective length required for efficient mixing and combustion of propellants. In practical terms, L* is an empirical measure used to ensure that the combustion chamber has sufficient volume and residence time for the propellants to mix, ignite, and burn completely before reaching the nozzle throat. Typical values of L* vary depending on the propellant combination and combustion chamber design, generally ranging from 0.8 to 1.6 meters for liquid-propellant thruster engines.

With an assumed characteristic length L*=0.8m, we obtain:

$$V_C = 0.8 \times 1.2246 \times 10^{-3} = 9.7966 \times 10^{-4}\ m^3$$

3.6.3 Propellant Stay Time in the Combustion Chamber

The propellant stay time ts in the combustion chamber is a crucial parameter for ensuring proper combustion. It is determined by the relationship:

$$t_s = \frac{V_C}{\dot{m} \times v} \tag{3-19}$$

Where:

v is the specific volume of the propellant, calculated using combustion chamber pressure, chamber temperature, and molecular weight obtained from NASA CEA.

The specific volume v is derived from the ideal gas law:

$$v = \frac{\mathrm{RT}}{\mathrm{P_C}} \tag{3-20}$$

Where:

- R is the specific gas constant, calculated using the universal gas constant Ru=8314 J/(kmol.K) and the molecular weight MW=21.121 kg/kmol from NASA CEA:

$$\mathrm{R} = \frac{\mathrm{R_u}}{\mathrm{MW}} = \frac{8314}{21.121} = 393.64\ \mathrm{J/kg.K} \tag{3-21}$$

- T=3384.02 K is the chamber temperature from NASA CEA.
- P_C=300 psia=2.068×10^6 Pa is the chamber pressure.

Now, substituting values into the specific volume equation:

$$v = \frac{393.64 \times 3384.02}{2.068 \times 10^6} = 0.644\ \mathrm{m^3/kg} \tag{3-22}$$

substituting values into the propellant stay time ts equation:

$$t_s = \frac{9.7966 \times 10^{-4}}{1.39 \times 0.644} = 1.09 \times 10^{-3} s = 1.09\ ms \tag{3-23}$$

This value demonstrates that the propellant remains in the chamber for an adequate amount of time to allow for complete mixing and combustion.

3.6.4 Combustion Chamber Length

Using the calculated chamber volume and area, the combustion chamber length Lc is derived as:

$$L_C = \frac{V_C}{A_C} = \frac{9.7966 \times 10^{-4}}{4.8983 \times 10^{-3}} = 0.2\ m = 20\ cm \tag{3-24}$$

3.7 RPA Results Interpretation

To confirm the validity of the design parameters obtained from NASA CEA, we used the Rocket Propulsion Analysis (RPA) software. The RPA provided additional design parameters and confirmed the consistency of the key performance metrics, such as thrust, specific impulse, mass flow rates, and chamber geometry. The results from RPA align closely with those calculated using NASA CEA, providing confidence in the accuracy and reliability of the design.

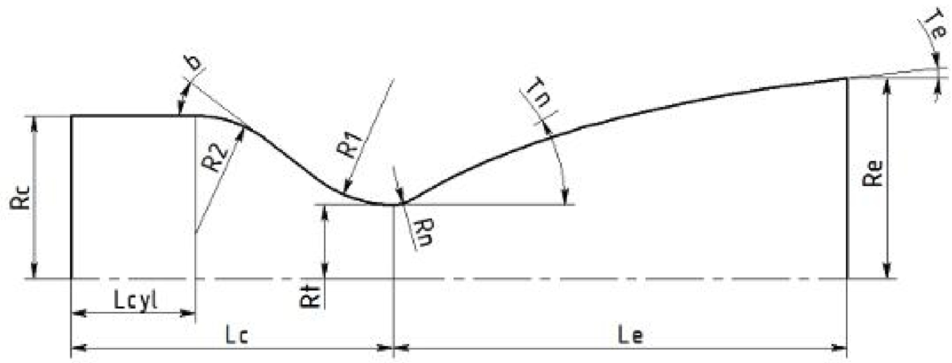

Figure 3.3 Design parameters by RPA tool

Thrust and mass flow rates			
Chamber thrust (vac)		5 kN	
Specific impulse (vac)		362.46736 s	
Chamber thrust (opt)		4.79335 N	
Specific impulse (opt)		347.48677 s	
Total mass flow rate		1.40663 kg/s	
Oxidizer mass flow rate		1.08102 kg/s	
Fuel mass flow rate		0.32561 kg/s	
Geometry of thrust chamber with parabolic nozzle			
Dc	78.77 mm	Le	474.39 mm
b	30 deg	Te	10.52 deg
R2	58.73 mm	De	393.87 mm
R1	29.54 mm	Ae/At	100
L*	800 mm	Le/Dt	12.04
Lc	221.62 mm	Le/c15 relative to length of cone nozzle with Te=15 deg	71.61 %

Lcyl	163.86 mm	Mass	9.06 kg
Dt	39.39 mm	Divergence efficiency	0.98417
Rn	7.52 mm	Drag efficiency	0.99157
Tn	38.84 deg	Thrust coefficient	2.00888 (vac)

Table 3-2 Geometry of Thrust Chamber with Parabolic Nozzle by RPA tool

These geometric parameters from RPA closely match those calculated through NASA CEA, further verifying the consistency and correctness of the design.

The data obtained from RPA thus confirms the performance predictions and supports the validity of the parameters used for the LOX/LCH_4 thruster engine design. This alignment enhances the confidence in our engine's expected behavior and performance during orbital transfer missions.

Chamber Performance

Thermodynamic properties | Performance | Altitude performance | Throttled performance

Thermodynamic properties (O/F=3.320)

Parameter	Injector	Nozzle inlet	Nozzle throat	Nozzle exit	Unit
Pressure	2.0684	2.0168	1.1848	0.0016	MPa
Temperature	3384.0145	3378.6817	3228.9549	1468.1145	K
Enthalpy	-1599.2878	-1616.3146	-2303.1804	-8067.8605	kJ/kg
Entropy	12.7334	12.7383	12.7383	12.7383	kJ/(kg·K)
Internal energy	-2931.4055	-2946.1026	-3557.1059	-8596.2680	kJ/kg
Specific heat (p=const)	8.2198	8.2300	7.9934	2.1096	kJ/(kg·K)
Specific heat (V=const)	7.0007	7.0106	6.8594	1.7495	kJ/(kg·K)
Gamma	1.1741	1.1739	1.1653	1.2059	
Isentropic exponent	1.1258	1.1257	1.1227	1.2059	
Gas constant	0.3937	0.3936	0.3883	0.3599	kJ/(kg·K)
Molecular weight (M)	21.1215	21.1251	21.4104	23.1007	
Molecular weight (MW)	0.02112	0.02113	0.02141	0.0231	
Density	1.5527	1.5166	0.9449	0.0031	kg/m^3
Sonic velocity	1224.6454	1223.4965	1186.5014	798.2384	m/s
Velocity	0.0000	184.5360	1186.5014	3596.8244	m/s
Mach number	0.0000	0.1508	1.0000	4.5060	
Area ratio	4.0000	4.0000	1.0000	100.0000	
Mass flux	279.8706	279.8706	1121.1271	11.2163	$kg/(m^2·s)$
Mass flux (relative)	1.353e-04	1.388e-04			kg/(N·s)
Viscosity	0.0001087	0.0001086	0.0001055	6.063e-05	kg/(m·s)
Conductivity, frozen	0.3793	0.3788	0.3631	0.1694	W/(m·K)
Specific heat (p=const), frozen	2.335	2.335	2.324	2.012	kJ/(kg·K)
Prandtl number, frozen	0.6692	0.6693	0.6749	0.7201	
Conductivity, effective	1.75	1.751	1.629	0.1708	W/(m·K)
Specific heat (p=const), effective	8.22	8.23	7.993	2.017	kJ/(kg·K)

Table 3-3 Thermodynamics properties by RPA tool

Chamber Performance

Thermodynamic properties | Performance | Altitude performance | Throttled performance

Theoretical (ideal) performance (O/F=3.320)

Parameter	Sea level	Sea level (flow sep.)	Optimum expansion	Vacuum	Unit
Characteristic velocity			1822.05		m/s
Effective exhaust velocity	-5289.98	337.45	3596.82	3743.73	m/s
Specific impulse (by mass)	-5289.98	337.45	3596.82	3743.73	N·s/kg
Specific impulse (by weight)	-539.43	34.41	366.77	381.75	s
Thrust coefficient	-2.9033	0.1852	1.9741	2.0547	

Estimated delivered performance (O/F=3.320)

Reaction efficiency: 0.9711

Nozzle efficiency: 0.9777

Overall efficiency: 0.9495

Parameter	Sea level	Sea level (flow sep.)	Optimum expansion	Vacuum	Unit
Characteristic velocity			1769.44		m/s
Effective exhaust velocity	-5479.12	168.74	3407.68	3554.59	m/s
Specific impulse (by mass)	-5479.12	168.74	3407.68	3554.59	N·s/kg
Specific impulse (by weight)	-558.71	17.21	347.49	362.47	s
Thrust coefficient	-3.0965	0.0954	1.9258	2.0089	

Ambient condition for optimum expansion: H=27.87 km, p=0.016 atm

Table 3-4 performance parameters by RPA tool

3.8 Thrust chamber Design using FreeCAD

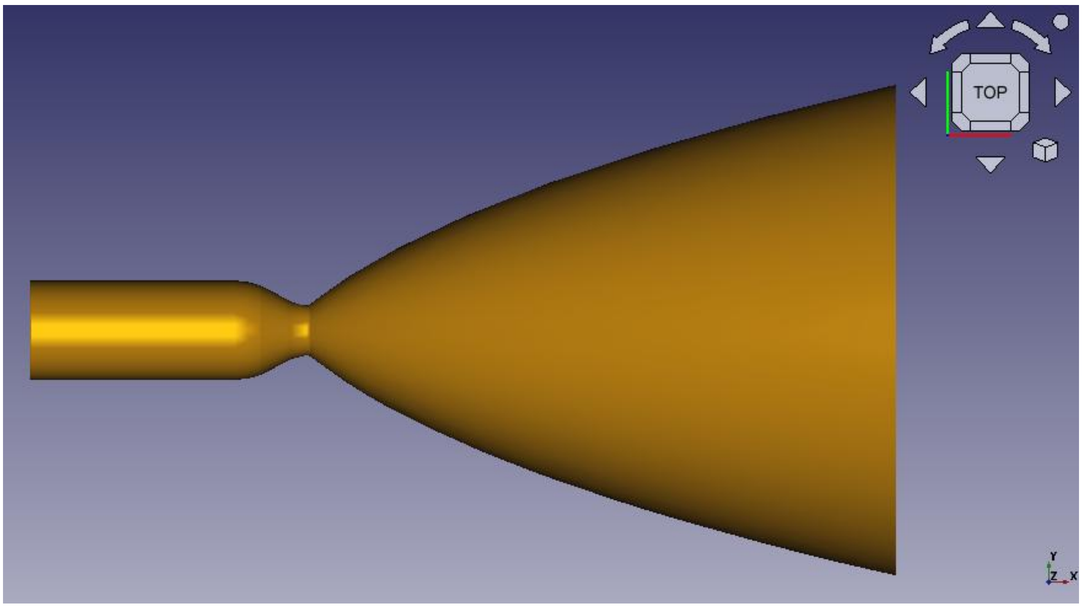

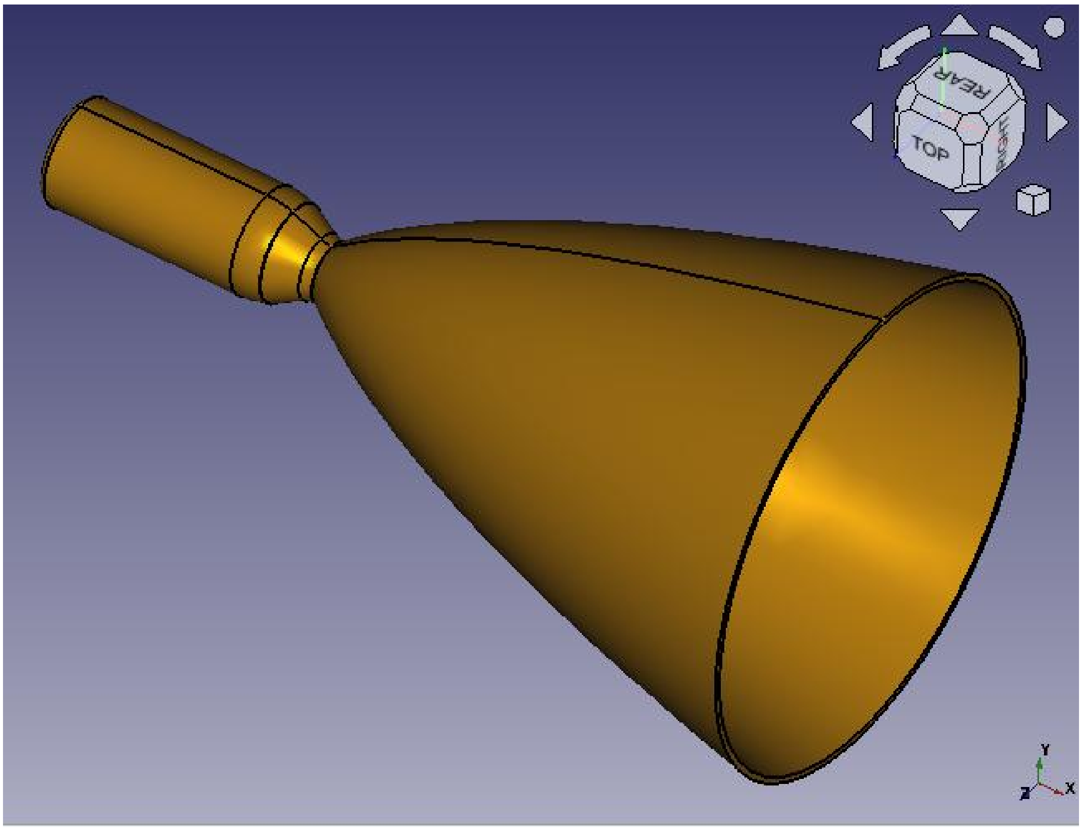

Figure 3.4 Thrust Chamber Design using FreeCAD

4 Fuel Requirements for Orbit Change

This chapter outlines the calculations required to determine the propellant mass and volumes for a spacecraft transferring from Low Earth Orbit (LEO) to Geostationary Earth Orbit (GEO). The analysis leverages the Tsiolkovsky rocket equation, using key parameters such as the required velocity change (Δv), specific impulse (Isp), and spacecraft masses. The chapter also includes calculations of the oxidizer and fuel mass proportions based on the mixture ratio and their respective volumes using density values. Finally, the burn time (tb) is computed to evaluate the operational feasibility of the LOX/LCH_4 thruster engine for this mission

4.1 Project Requirements

- Δv (velocity change required): 4000 m/s
- Payload mass: 50 kg

4.2 Key Parameters

- Specific Impulse (Isp): 366.69 seconds (according to design in chapter 3)
- Dry mass (structure + tanks + engine): 60 kg (estimation based on design in chapter 3)
- Total mass without propellant (dry mass + payload mass): 110 kg
- Oxidizer/Fuel Mixture Ratio: MR = 3.32 (mass ratio of LOX to LCH4)
- Densities:
  - Liquid Oxygen (LOX): $\rho_{\mathrm{LO_2}} = 1.141\ \mathrm{kg}/\ell$
  - Liquid Methane (LCH4): $\rho_{\mathrm{LCH_4}} = 0.422\ \mathrm{kg}/\ell$

4.3 Tsiolkovsky Equation

The rocket equation, also known as the **Tsiolkovsky rocket equation**, is used to relate the change in velocity (Δv) to the ratio of the initial mass (m_i) and final mass (m_f) of the spacecraft. The equation is as follows:

$$\Delta \mathrm{v} = \mathrm{I_{sp}} \times \mathrm{g_0} \times \ln\left(\frac{\mathrm{m_i}}{\mathrm{m_f}}\right) \tag{4-1}$$

Where:

$\mathrm{g_0}$ = 9.81 m/s² (standard gravitational acceleration)

$\mathrm{m_i}$= initial mass (spacecraft mass including fuel)

$\mathrm{m_f}$ = final mass (spacecraft mass without fuel, i.e., dry mass + payload mass)

4.4 Propellant mass Calculations

Rearranging the rocket equation to solve for the initial mass $\mathrm{m_i}$:

$$m_i = m_f \times e^{\frac{\Delta \mathrm{v}}{\mathrm{I_{sp}} \times \mathrm{g_0}}} \tag{4-2}$$

Substituting the known values:

$$m_i = 110 \times e^{\frac{4000}{366.69 \times 9.81}} \approx 334.44\, kg \tag{4-3}$$

The total propellant mass is the difference between the initial mass and the final mass:

$$\text{Propellant Mass} = \mathrm{M_P} = m_i - m_f = 334.44\text{ kg} - 110\text{ kg} = 224.44\text{ kg} \tag{4-4}$$

Since the oxidizer-to-fuel mixture ratio is 3.45, the masses of liquid oxygen (LOX) and liquid methane (LCH4) can be calculated as follows:

$$\text{Oxidizer Mass} = \frac{\mathrm{M_P} \times \mathrm{MR}}{1 + \mathrm{MR}} \tag{4-5}$$

$$\text{Oxidizer Mass} = \mathrm{M_{LO_2}} = \frac{224.44 \times 3.32}{1 + 3.32} = 172.48\text{ kg}$$

$$\text{Fuel Mass} = \frac{\mathrm{M_P}}{1 + \mathrm{MR}} \tag{4-6}$$

$$\text{Fuel Mass} = \mathrm{M_{LCH_4}} = \frac{224.44}{1 + 3.32} = 51.95\text{ kg}$$

4.5 Propellant Volume Calculations

To convert the propellant masses to volume, we use their respective densities:

- **Liquid Oxygen (LOX) Volume:**

$$V_{LO_2} = \frac{\mathrm{M_{LO_2}}}{\rho_{\mathrm{LO_2}}} = \frac{172.48\, kg}{1.141\, kg/\ell} \approx 151.17\ell \tag{4-7}$$

- **Liquid Methane (LCH4) Volume:**

$$V_{LCH_4} = \frac{\mathrm{M_{LCH_4}}}{\rho_{\mathrm{LCH_4}}} = \frac{51.95\, kg}{0.422\, kg/\ell} \approx 123.11\, \ell \tag{4-8}$$

4.6 Burn Time

The burn time tb is a critical parameter in evaluating the feasibility of the orbit transfer mission that connects mission requirements and engine performance. It reflects the duration the thruster must operate to achieve the required Δv for the transfer from LEO-to-GEO while ensuring efficient use of propellants.

The burn time is calculated using the relation:

$$t_b = \frac{M_P}{\dot{m}} = \frac{224.44\, kg}{1.39\, kg/s} = 161.47\, s = 2\, minutes\, 41.47s \tag{4-9}$$

4.6.1 Mission-Level Analysis

From a mission perspective:

- The burn time aligns with the Δv requirement, confirming that the engine can sustain operation for the duration needed to complete the orbit transfer maneuver.

- The calculated tb ensures sufficient propellant is available, eliminating the risk of fuel depletion.
- This duration allows precise and controlled execution of the orbit transfer, meeting the mission's overall objectives.

4.6.2 Engine Performance Analysis

From an engine performance perspective:

- The burn time validates the thruster’s ability to maintain the required thrust and mass flow over the specified duration.
- Combustion stability is confirmed by the propellant stay time (ts) (1.09 ms), which is significantly shorter than tb. This indicates that the combustion chamber design ensures complete mixing and combustion within the chamber before expulsion through the nozzle.
- The chamber pressure of 300 psia and the designed mass flow rate align with the calculated burn time, verifying the engine’s efficiency in utilizing the propellants.

4.7 Conclusion

The calculations presented in this chapter validate the feasibility of the LEO-to-GEO orbit transfer using the LOX/LCH_4 thruster engine. The propellant mass of 224.44 kg meets the mission's Δv requirement, with oxidizer and fuel volumes well within practical storage limits. A burn time of approximately 161.47 seconds confirms that the engine can sustain the required operation to execute the maneuver, while maintaining efficiency and stability in combustion. These results demonstrate the engine’s capability to fulfill mission objectives and provide a solid foundation for subsequent design and operational considerations.

5 Thermal Analysis of LOX/LCH4 Thrust Chamber with Regenerative Cooling

This section details the thermal analysis of the LOX/LCH4 thruster engine's thrust chamber, focusing on the implementation of a regenerative cooling system. The design was analyzed using RPA software, incorporating various critical parameters such as wall material, coolant properties, and channel geometry to evaluate the thermal performance and ensure the structural integrity of the thrust chamber under operational conditions.

5.1 Methodology and Inputs

Regenerative cooling is the most widely used method of cooling a thrust chamber and is accomplished by flowing high-velocity coolant over the back side of the chamber hot gas wall to convectively cool the hot liner. The coolant with the heat input from cooling the liner is then usually discharged into the injector and utilized as a propellant.

The regenerative cooling system employs liquid methane (LCH_4) as the coolant due to its favorable thermodynamic properties.

Configuration of the regenerative cooling segment includes the following parameters:

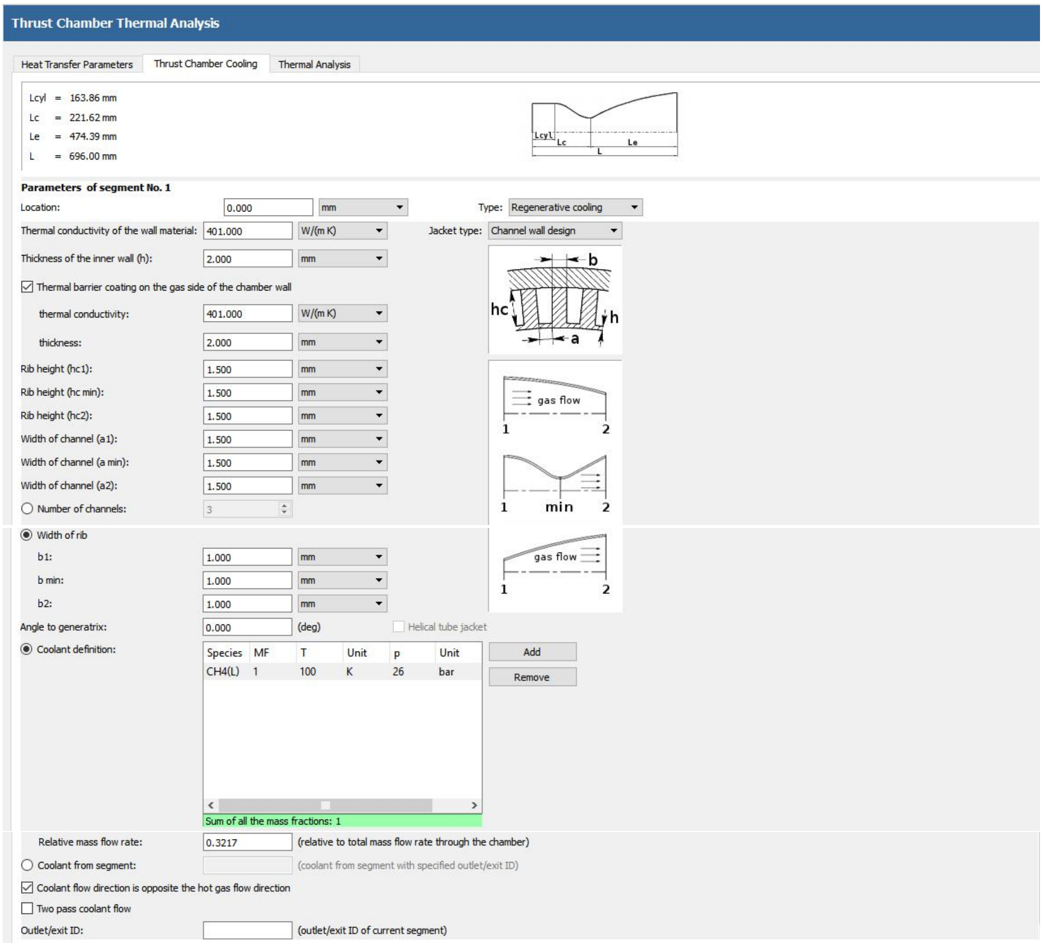

The regenerative cooling approach ensures efficient heat transfer between the chamber wall and the coolant, leveraging the high thermal conductivity of copper to maintain structural and thermal integrity.

The selection of initial pressure and temperature for the cooling system is based on operational requirements and thermodynamic considerations:

- **Initial Pressure (26 bar):**

The combustion chamber pressure is set at 300 psia (approximately 20.68 bar). To ensure sufficient pressure for liquid methane at the injector inlet, the pressure of the coolant at the cooling pipe outlet is set at 22 bar. Assuming a pressure drop of 2 bar in the injector, this configuration ensures proper flow into the combustion chamber.

A pressure drop of approximately 4 bar is expected across the cooling pipes. Consequently, the initial pressure of liquid methane at the cooling pipe inlet is set at 26 bar.

Since the methane is stored at atmospheric pressure (1 bar) in the fuel tank, it must be pressurized to 26 bar using helium before entering the cooling pipes.

- **Initial Temperature (100 K):**

Using the methane phase diagram (Figure 5.), the boiling point of methane at 26 bar is approximately 173 K, and the freezing point is approximately 91 K. To avoid phase change within the cooling pipes, the initial temperature of the liquid methane at the inlet is chosen to be higher than the freezing point. The selected temperature of 100 K ensures that the coolant remains in liquid form throughout the cooling process.

As the coolant absorbs heat in the cooling pipes, its temperature will increase to above the boiling point (173 K) before entering the combustion chamber, ensuring efficient heat absorption and proper injection as a gaseous propellant.

This careful selection of pressure and temperature parameters ensures the stability, efficiency, and reliability of the regenerative cooling system under the specified operational conditions.

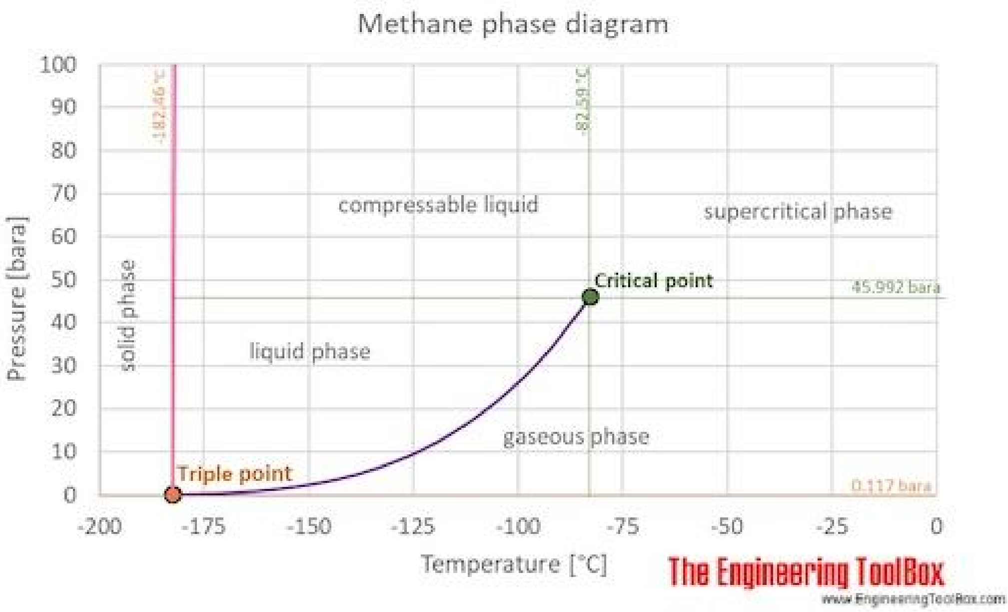

Figure 5.1 Methane phase diagram

5.2 Results and Observations

The results of the RPA thermal analysis include critical thermal and flow parameters distributed along the thrust chamber. Key metrics are summarized in Table 5-1, providing insights into the chamber's thermal performance and the efficiency of the regenerative cooling system.

5.2.1 Key Parameters

- Location (mm): The axial distance along the cooling channel.
- Radius (mm): The radial position of the point of analysis.
- Convective Heat Transfer Coefficient (W/m²-K): Indicates the efficiency of heat transfer between the coolant and the wall.
- Convective Heat Flux (kW/m²): Heat flux attributed to convection from the gas-side wall to the coolant.
- Radiative Heat Flux (kW/m²): Heat flux due to radiation from the combustion gases to the chamber wall.
- Total Heat Flux (kW/m²): Combined heat flux from convection and radiation.
- T_{wg}, (K): the temperature of chamber wall on its hot gas side.
- Twi, (K): the temperature between the thermal barrier coating layer and chamber wall (if coating is available).
- T_{wc}, (K): the temperature of chamber wall on its cooler side.
- p_c (MPa), T_c , (K), w_c (m/s), ρ (kg/m³): the pressure, temperature, velocity, and density of the coolant correspondingly (if applicable).

Thrust Chamber Thermal Analysis

Heat Transfer Parameters | Thrust Chamber Cooling | Thermal Analysis

Results of steady-state thermal analysis at chamber throttle level R=1.000

Location, mm	Radius	Conv. heat coeff., kW/m^2-K	Conv. heat flux, kW/m^2	Rad. heat flux	Total heat flux	Twg, K	Twi, K	Twc, K	Tc, K	pc, MPa	wc, m/s	rho, kg/m^3	Comments
0.00	39.39	2.2204	5419.0424	369.5441	5788.5865	1101.65	1072.79	1043.92	598.46	2.296	199.62	7.33	regenerative cooling, opposite flow
10.24	39.39	2.2177	5397.4519	501.8724	5899.3243	1108.39	1078.96	1049.54	588.46	2.309	194.87	7.51	regenerative cooling, opposite flow
20.48	39.39	2.2157	5381.6192	604.4595	5986.0787	1113.37	1083.52	1053.66	578.17	2.321	190.23	7.70	regenerative cooling, opposite flow
30.72	39.39	2.2144	5371.1883	677.9497	6049.1379	1116.63	1086.46	1056.29	567.63	2.333	185.72	7.88	regenerative cooling, opposite flow
40.96	39.39	2.2138	5366.4461	722.1986	6088.6447	1118.13	1087.76	1057.39	556.88	2.345	181.33	8.07	regenerative cooling, opposite flow
51.21	39.39	2.2140	5367.8666	736.5216	6104.3882	1117.66	1087.18	1056.74	545.94	2.356	176.81	8.28	regenerative cooling, opposite flow
61.45	39.39	2.2146	5372.4771	736.7734	6109.2505	1116.22	1085.74	1055.27	534.84	2.367	172.01	8.51	regenerative cooling, opposite flow
71.69	39.39	2.2150	5375.7877	736.7342	6112.5219	1115.14	1084.61	1054.12	523.59	2.378	167.39	8.75	regenerative cooling, opposite flow
81.93	39.39	2.2152	5377.9539	737.1293	6115.0832	1114.46	1083.92	1053.42	512.18	2.388	162.95	8.99	regenerative cooling, opposite flow
92.17	39.39	2.2154	5378.8946	737.2670	6116.1616	1114.19	1083.66	1053.16	500.61	2.399	158.68	9.23	regenerative cooling, opposite flow
102.41	39.39	2.2155	5380.1238	737.4304	6117.5542	1113.80	1083.26	1052.74	488.87	2.408	153.76	9.52	regenerative cooling, opposite flow
112.65	39.39	2.2155	5380.0498	737.5160	6117.5658	1113.83	1083.30	1052.79	476.97	2.418	149.02	9.83	regenerative cooling, opposite flow
122.89	39.39	2.2152	5378.0220	737.0217	6115.0437	1114.40	1083.82	1053.32	464.89	2.427	144.50	10.13	regenerative cooling, opposite flow
133.13	39.39	2.2148	5374.6115	736.8000	6111.4115	1115.54	1085.03	1054.55	452.63	2.436	140.17	10.45	regenerative cooling, opposite flow
143.37	39.39	2.2144	5371.5847	736.3127	6107.8974	1116.45	1085.92	1055.46	440.19	2.444	135.20	10.83	regenerative cooling, opposite flow
153.62	39.39	2.2139	5367.3373	737.3523	6104.6897	1117.84	1087.38	1056.94	427.58	2.452	130.28	11.24	regenerative cooling, opposite flow
163.86	39.39	2.2130	5360.7789	736.1863	6096.9652	1119.83	1089.35	1058.94	414.78	2.460	125.64	11.65	regenerative cooling, opposite flow
176.42	38.03	2.3594	5685.3289	737.0024	6422.3313	1132.49	1100.44	1068.41	398.58	2.470	125.23	12.20	regenerative cooling, opposite flow
188.98	33.74	2.9393	6981.5572	723.6018	7705.1590	1166.55	1128.00	1089.57	380.43	2.482	136.00	13.00	regenerative cooling, opposite flow
201.55	26.71	4.5075	10393.4782	686.1074	11079.5855	1234.64	1179.33	1124.07	358.26	2.499	170.05	14.03	regenerative cooling, opposite flow
214.11	20.66	7.1421	15996.4388	509.8045	16506.2433	1294.21	1211.84	1129.52	333.32	2.529	218.43	15.62	regenerative cooling, opposite flow
221.62	19.69	7.6722	17115.1256	479.9472	17595.0728	1294.96	1207.18	1119.43	318.49	2.554	218.01	16.81	regenerative cooling, opposite flow
246.74	36.84	2.1600	5380.4762	86.7848	5467.2610	981.34	954.11	926.85	269.79	2.584	72.01	22.05	regenerative cooling, opposite flow
271.87	53.71	1.0235	2721.7401	51.4268	2773.1669	795.81	782.29	768.46	239.07	2.593	37.12	27.45	regenerative cooling, opposite flow
271.87	53.71	1.0235	2721.7401	51.4268	2773.1669	795.81	782.29	768.46	239.07	2.593	37.12	27.45	regenerative cooling, opposite flow
297.00	68.69	0.6275	1755.6752	36.2274	1791.9026	647.83	639.77	630.83	219.62	2.596	21.39	36.15	regenerative cooling, opposite flow
322.12	82.17	0.4405	1280.0616	26.9494	1307.0109	533.14	526.43	519.91	207.33	2.597	12.81	49.60	regenerative cooling, opposite flow
347.25	94.42	0.3318	976.4498	21.2432	997.6930	491.11	485.56	480.58	197.67	2.598	8.04	67.97	regenerative cooling, opposite flow
372.37	105.62	0.2648	782.4703	17.2756	799.7459	475.14	470.86	466.87	188.24	2.599	5.89	82.33	regenerative cooling, opposite flow
397.50	115.93	0.2188	651.7133	14.5079	666.2212	448.48	444.95	441.62	178.37	2.599	4.80	91.45	regenerative cooling, opposite flow
422.62	125.47	0.1872	561.8975	12.4208	574.3183	422.72	419.66	416.80	168.92	2.599	4.11	98.38	regenerative cooling, opposite flow
447.75	134.33	0.1639	495.3010	10.8938	506.1948	399.27	396.56	394.03	160.08	2.599	3.61	104.15	regenerative cooling, opposite flow
472.87	142.59	0.1461	444.5900	9.6953	454.2853	376.99	374.63	372.36	151.94	2.599	3.23	109.23	regenerative cooling, opposite flow
498.00	150.30	0.1333	411.1724	8.7764	419.9488	333.21	331.15	329.06	144.74	2.600	1.29	258.40	regenerative cooling, opposite flow
523.13	157.53	0.1224	380.7931	8.0227	388.8157	304.96	302.45	300.51	138.45	2.600	0.83	382.57	regenerative cooling, opposite flow
548.25	164.31	0.1127	351.6565	7.3625	359.0190	295.85	293.47	291.68	132.55	2.600	0.78	392.54	regenerative cooling, opposite flow
573.38	170.68	0.1047	327.3311	6.8147	334.1458	287.77	285.49	283.83	126.77	2.600	0.73	401.88	regenerative cooling, opposite flow
598.50	176.69	0.0979	306.7629	6.3980	313.1610	280.33	278.15	276.59	121.09	2.600	0.69	410.70	regenerative cooling, opposite flow
623.63	182.34	0.0921	289.0394	6.0023	295.0418	274.17	272.06	270.59	115.52	2.600	0.65	418.91	regenerative cooling, opposite flow
648.75	187.68	0.0871	273.8114	5.6067	279.4181	268.19	266.13	264.74	110.05	2.600	0.62	426.79	regenerative cooling, opposite flow
696.00	196.94	0.0793	249.8364	5.1104	254.9468	260.37	258.44	257.16	100.00	2.600	0.57	440.78	regenerative cooling, opposite flow

Table 5-1 Thermal Analysis Results from RPA for Regenerative Cooling with Direct Flow

5.2.2 Observations and Design Implications

The results presented in Table 5-1 highlight several significant trends and design implications for the engine's thermal management:

5.2.2.1 Interpretation of Heat Transfer Coefficient and Heat Flux

In thruster engine thermal analysis, the heat transfer coefficient (h) and heat flux (q) are critical parameters that characterize the cooling and heat dissipation performance:

- **Heat Transfer Coefficient (h):**

Represents the efficiency of heat exchange between the hot gases inside the combustion chamber and the chamber wall.

Higher values indicate more effective heat transfer, which may require robust cooling mechanisms to prevent material failure.

In the presented results in table 5-1, h remains relatively constant along the regenerative cooling flow path, with slight variations indicating the influence of flow properties and chamber geometry.

- **Convective Heat Flux (q_{conv}):**

Quantifies the heat transferred per unit area from the hot gases to the wall via convection.

Calculated as:

$$q_{Conv} = h \,.\, (T_{gas} - T_{wall}) \tag{5-1}$$

where T_{gas} is the combustion gas temperature, and T_{wall} is the inner wall temperature.

High q_{conv} values near the throat region highlight the need for enhanced cooling as gas velocity and temperature peak in this area.

- **Radiative Heat Flux (q_{rad}):**

Results from thermal radiation emitted by the hot gases, described by:

$$q_{rad} = \varepsilon \,.\, \sigma \,.\, T_{gas}^4 \tag{5-2}$$

where ϵ is the emissivity, and σ is the Stefan-Boltzmann constant.

Comparatively smaller than q_{conv} but still contributes to the overall heat load.

- **Total Heat Flux (q_{total}):**

Summation of convective and radiative components:

$$q_{total}=q_{conv}+q_{rad} \tag{5-3}$$

Represents the overall thermal stress on the cooling system and chamber walls. Regions with high q_{total} require sufficient cooling capacity to maintain structural integrity.

Observations

The heat transfer coefficient decreases slightly along the flow direction, corresponding to reduced gas temperatures and changing flow characteristics. (Figure 5.2)

Convective heat flux values are highest near the throat (10,595 kW/m²) due to the combination of high temperatures and gas velocities.

Radiative heat flux becomes significant where gas temperatures remain elevated, particularly in the combustion zone.

The total heat flux peaks in the throat area and gradually diminishes downstream, corresponding to decreasing temperatures and expanding flow in the nozzle.

These results underline the importance of an optimized regenerative cooling design, especially near the throat and combustion chamber regions, where thermal loads are most severe.

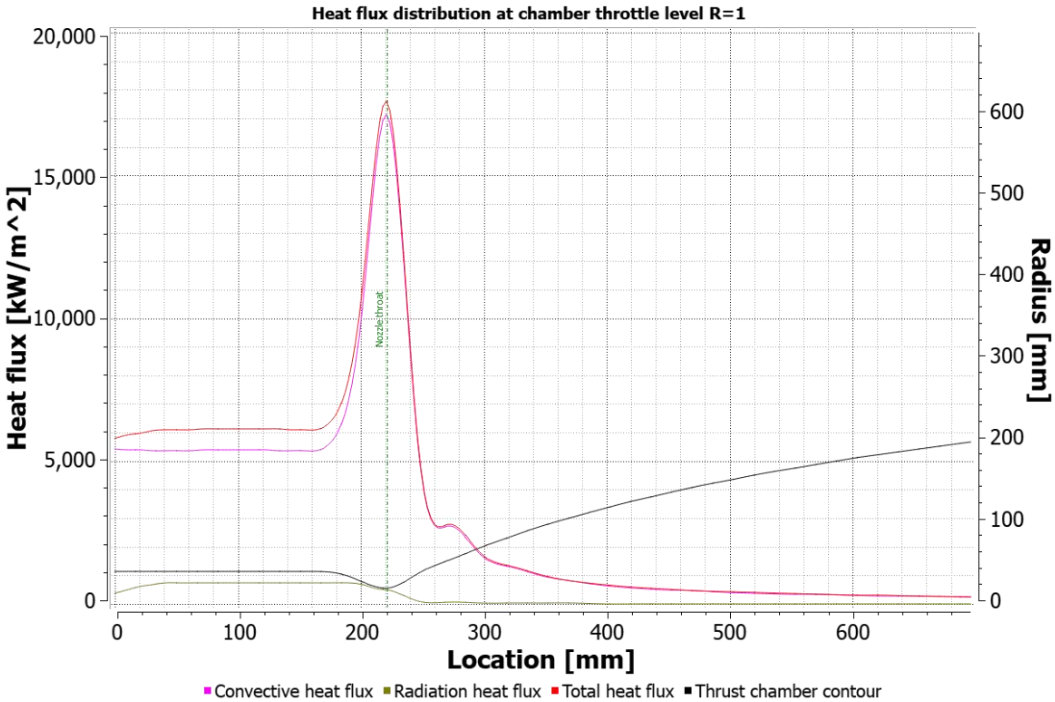

Figure 5.2 RPA-Generated Variation of Convective, Radiation, and Total Heat Flux with Axial Location and Radius, Emphasizing the Significant Flux at the Throat

5.2.2.2 Coolant Temperature

In the coolant system design for the thruster, it is observed that the coolant reaches its boiling point before entering the combustion chamber. As shown in Figure 5-3 and detailed in Table 5-1, the coolant temperature (Tc) increases within the coolant pipes, ultimately achieving its boiling point. This phenomenon is particularly advantageous as it ensures that the coolant undergoes a phase change to gas prior to entering the combustion chamber. The transition to gas enhances heat transfer efficiency, as the latent heat of vaporization facilitates effective cooling. This thermal behavior is beneficial for maintaining optimal operating conditions for the thruster and preventing overheating of critical components.

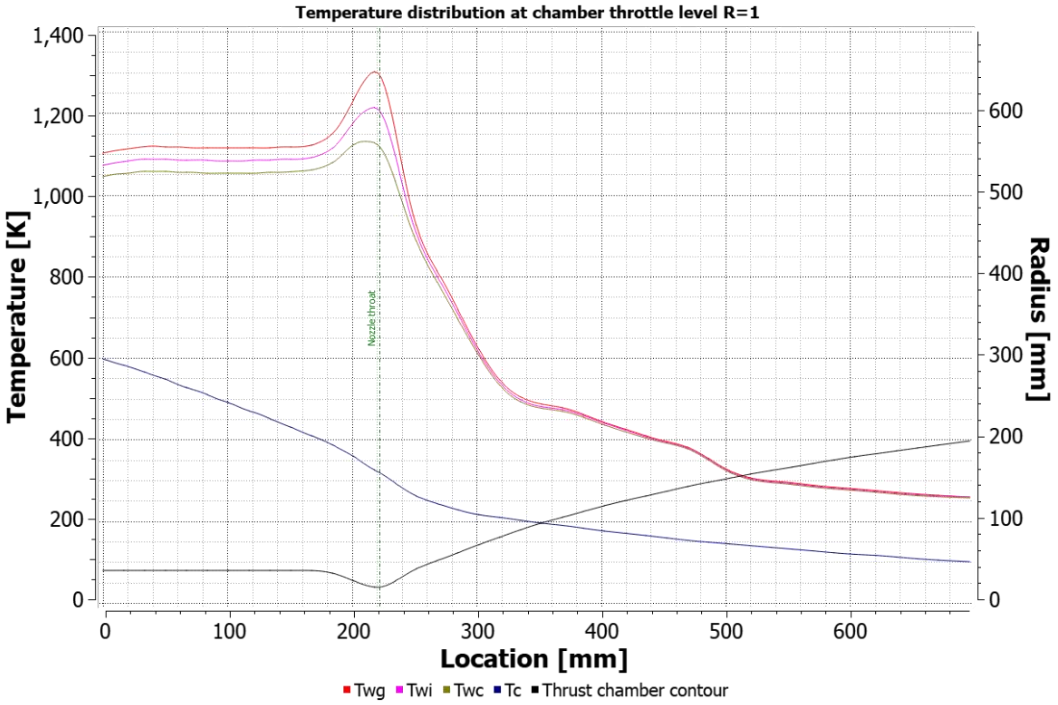

Figure 5.3 RPA-Generated Variation of T_{wg}, T_{wi}, T_{wc} and T_C with Radius and Axial Location in the Thrust Chamber

5.2.2.3 Wall Temperatures:

- The gas-side wall temperature (T_{wg}) is highest near the throat, reaching a peak of approximately 1,294 K. This observation reflects the intense thermal loading at this location due to high flow velocities and reduced cross-sectional area.
- The coolant-side wall temperature (T_{wc}) is significantly lower than gas-side wall temperature, reflecting the effectiveness of the cooling mechanism. Figure 5-3 depicts the temperature distribution across the radius and length, highlighting the critical thermal gradient at the throat region.

5.2.2.4 Structural Integrity and Material Selection

The structural integrity of the wall materials must accommodate elevated temperatures observed in the combustion chamber and nozzle. This necessitates the selection of materials with high melting points, excellent thermal conductivity, and robust mechanical properties under extreme conditions. In this context, copper and its alloys are commonly preferred due to their favorable properties, including high thermal conductivity and adequate melting points.

Melting Point of Copper at Elevated Pressure

The melting point of copper (Cu) increases slightly under elevated pressures, such as the 300 psia (approximately 20.7 bar) operational conditions in the combustion chamber. This behavior can be analyzed using the Clausius-Clapeyron relation, which estimates the shift in melting point with pressure:

$$\frac{dT}{dP} = \frac{T_m \cdot \Delta v}{\Delta H_f} \tag{5-4}$$

Where:

T_m: Melting temperature in kelvin at standard pressure (1357.77 K).

Δv: Change in specific volume during melting ($v_{liquid} - v_{solid} = 1.31 \times 10^{-5} \mathrm{m}^3/\mathrm{kg}$).

ΔH_f: Latent heat of fusion (13.05kJ/mol, equivalent to 205 kJ/kg for copper).

dT/dP: Rate of change of melting temperature with pressure.

- **Standard Melting Point:**

At 1 atm pressure, the melting point of copper is 1357.77 K (1084.62°C).

- **Effect of Pressure:**
  For the given conditions:

$$\frac{dT}{dP} = \frac{1357.77 \times 1.31 \times 10^{-5}}{205 \times 10^{3}} = 8.7 \times 10^{-8} \, {}^{K}/_{Pa} \tag{5-5}$$

With a pressure increase of ΔP=19.7bar = 197x 10^4 Pa.

$\Delta T_m \approx 0.171$k

- **Resulting Melting Point:**

The new melting point under 300 psia pressure becomes:

$$T_m^{'} = 0.171 + 1357.77 = 1357.94\,K \tag{5-6}$$

Comparison with Wall Temperatures

The calculated melting point of copper under 300 psia, approximately 1357.94 K, is significantly higher than the highest observed inner wall temperature near the throat region (1294.96 K). This confirms that copper-based materials can maintain their structural integrity under the operating conditions.

Implications for Design

Material Suitability: Copper and its alloys are suitable for the combustion chamber and nozzle due to their ability to withstand extreme thermal conditions without reaching their melting point.

Thermal Management: High thermal conductivity of copper facilitates efficient heat dissipation, reducing thermal gradients and stress across the wall.

Safety Margin: The melting point margin ensures operational reliability and durability, even in the most thermally critical regions.

In conclusion, the selection of copper or its high-temperature alloys, potentially enhanced with thermal barrier coatings, provides a robust solution to manage the thermal and structural demands of the thruster engine.

These observations underscore the importance of detailed thermal analysis in guiding the design and optimization of the thruster's regenerative cooling system. The data provides a foundation for selecting materials, optimizing cooling channel geometry, and ensuring the overall thermal reliability of the propulsion system.

6 Prototype and Test Stand Realization

This chapter presents the process of prototyping and test stand realization for the LOX/LCH_4 thruster engine. It includes visual documentation of the combustion chamber and nozzle manufacturing stages, the integration into the orbit change test stand, examples of commercially available components, and considerations for regenerative cooling.

6.1 Plastic Model of Combustion Chamber and Nozzle from 3D Printer

The initial stage involved fabricating a plastic model of the combustion chamber and nozzle using a 3D printer. This model served as the basis for creating a sand mold to be used in the copper casting process (Figures 6.1).

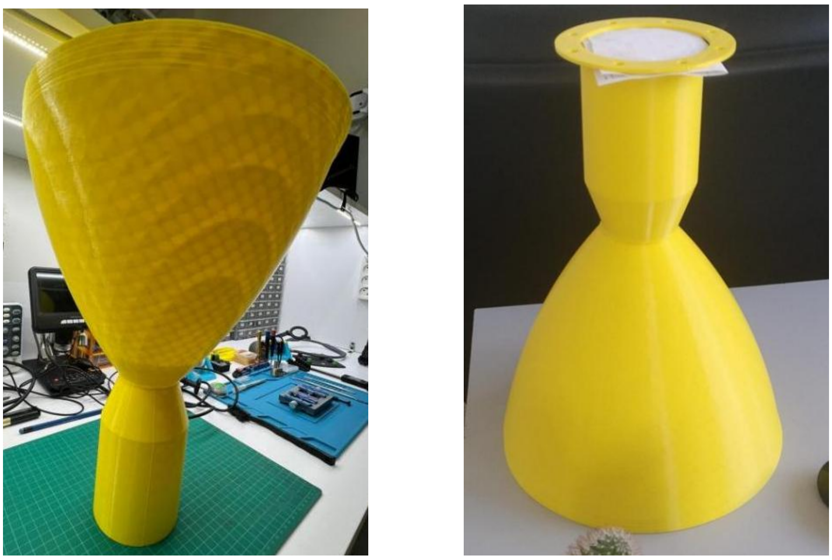

Figure 6.1 Plastic Model of the Combustion Chamber and Nozzle Fabricated at AECENAR

6.2 Combustion Chamber and Nozzle After Melting and Forming Copper

Following the sand mold preparation, the combustion chamber and nozzle were cast in copper. This process ensured the high thermal conductivity required for effective heat dissipation during operation.(Figures 6.2)

Figure 6.2 Copper-Formed Combustion Chamber and Nozzle Fabricated at AECENAR

6.3 Integration into Orbit Change Test Stand

The copper combustion chamber and nozzle were subsequently integrated into the orbit change test stand. This setup forms the foundation for testing the thruster engine under controlled conditions (Figure 6.3).

Figure 6.3 Integration of the Copper Thrust Chamber into the Orbit Change Test Stand at AECENAR

6.3.1 Examples of Commercially Available Components

In the context of designing and realizing the test stand, understanding commercially available hardware helps to evaluate practical implementation possibilities. One such example is an oxidizer tank designed for 45 liters of LOX, photographed in Germany (Figure 6.4).

While this tank does not meet the specific requirements of our design, it provides insight into critical parameters for component selection, including:

- Capacity: 45 liters of LOX, equivalent to approximately 90 kg.
- Wall Thickness: Approximately 10 cm, designed to insulate -193°C storage conditions.
- Cost:
  - Empty tank: 6000 EUR
  - Filling cost: 670 EUR
- Manufacturer: Linde, commonly used for medical applications.

Including real-world examples such as this strengthens our understanding of available solutions and provides a foundation for future improvements to our design.

Figure 6.4 Oxidizer Tank Designed for 45 Liters of LOX, Photographed in Germany

6.4 Regenerative Cooling

6.4.1 Structure of Regenerative Cooling System

The regenerative cooling system is essential for managing the intense thermal environment within the combustion chamber and nozzle. It is typically structured as a three-layer "sandwich" arrangement, each layer playing a distinct role in heat management.

- **Innermost Layer – Hot Gas Wall:**
  The innermost layer is the hot gas wall, which is directly exposed to the combustion gases. This wall absorbs the extreme heat generated by the combustion process and is subjected to high thermal stresses. The material selected for this layer must possess high thermal conductivity to transfer heat effectively while withstanding the harsh conditions of the combustion chamber (Figure 6.2)
- **Middle Layer – Cooling Channels:**
  Surrounding the hot gas wall is the cooling channel layer, which is discussed in Section 6.4.2. This layer contains the channels through which the coolant (typically the propellants) flows. The coolant absorbs heat from the hot gas wall as it passes through these channels, ensuring that the combustion chamber and nozzle remain within safe temperature limits. The design of these channels is critical for efficient heat transfer and for preventing hot spots that could damage the chamber (Fgures 6.5).
- **Outermost Layer – Closeout Wall:**
  The outermost layer is the closeout wall, which seals the cooling system and keeps the coolant within the channels. This layer also protects the structural integrity of the engine by providing an outer casing that prevents coolant leakage and maintains pressure within the cooling system. The closeout wall is designed to withstand external stresses and environmental conditions while supporting the efficient operation of the cooling system.

6.4.2 Realization of pipes layout

The design and layout of the regenerative cooling pipes are critical to ensuring the structural integrity and thermal efficiency of the combustion chamber and nozzle. This section highlights the integration of cooling pipes, including the incorporation of inlets and outlets for the propellants—fuel and oxidizer—designed to pass through the cooling system. The proper arrangement of these pipes allows for optimal heat dissipation, preventing excessive thermal stress on the engine components.

Figure 6.5 Realization of Pipes Layout for Regenerative Cooling

Figure 6.6 Thrust Chamber After Integration of Propellant Inlets and Outlets for Regenerative Cooling

6.4.3 Outermost Layer – Closeout Wall

The closeout wall is the outermost layer of the regenerative cooling system, serving to seal the cooling channels and contain the coolant. It is designed to withstand external stresses, pressure buildup, and environmental factors, ensuring the integrity of the cooling system. Made from high-strength, thermally resistant materials, the closeout wall prevents coolant leakage and protects the system from mechanical vibrations and temperature extremes. Figures in this section illustrate the integration of the closeout wall.

Figure 6.7 Integration of the Closeout Wall into the Regenerative Cooling System at AECENAR

7 Conclusion

In conclusion, this thesis has made significant contributions to the design, analysis, and realization of a LOX/LCH_4 thruster engine for spacecraft propulsion, with a focus on the transfer from Low Earth Orbit (LEO) to Geostationary Earth Orbit (GEO). Through the use of advanced simulation tools such as NASA CEA and RPA, we optimized critical design parameters, including the stoichiometric and optimal mixture ratios, nozzle geometry, combustion chamber dimensions, and fuel requirements, ensuring the propulsion system meets mission objectives.

The successful design of the combustion chamber and nozzle, coupled with the integration of regenerative cooling, demonstrated the feasibility of the system under expected thermal and structural conditions. The comprehensive calculations for thrust, mass flow rates, and burn time, supported by a prototype test stand, underscore the practical potential for real-world implementation.

This work not only advances our understanding of LOX/LCH_4 propulsion systems but also contributes to the broader field of space propulsion technology. The results presented provide a solid foundation for further optimization and experimental validation of the design. Future research should focus on the experimental testing of the propulsion system to confirm its performance and address any challenges encountered during implementation.

Moreover, the insights gained from this study have broader implications for space exploration, where efficient propulsion systems are critical for reducing mission costs and improving the reliability of space travel. As the space industry continues to evolve, the findings of this thesis align with efforts to enhance propulsion systems, making space missions more sustainable and cost-effective.

In summary, this thesis provides a comprehensive approach to the design and optimization of LOX/LCH_4 thruster engines, contributing valuable knowledge to the field of space propulsion and laying the groundwork for future advancements in spacecraft propulsion systems.

Bibliography

[1] M. J. Casiano, J. R. Hulka und V. Yang, „Liquid-Propellant Rocket Engine Throttling: A Comprehensive Review,“ *Journal of Propulsion and Power,* pp. 897-923, 09/2010.

[2] D. Krejci und P. Lozano, „Space Propulsion Technology for Small Spacecraft,“ Chicago, IL, USA, 3/2018.

[3] D. K. Huzel und D. H. Huang, Modern Engineering for Design of Liquid-Propellant Rocket Engines, Washington DC: American Institute of Aeronautics and Astronautics, 1992-01-01, p. 467.

[4] G. P. Sutton und O. Biblarz, Rocket Propulsion Elements, 9th Hrsg., Hoboken, New Jersey: John Wiley & Sons, 2017, p. 791.

[5] D. P. Mishra, Fundamentals of rocket propulsion, Boca Raton: CRC Press, Taylor & Francis Group, CRC Press is an imprint of the Taylor & Francis Group, an informa business, 2017, p. 461.

[6] A. De Iaco Veris, Fundamental Concepts of Liquid-Propellant Rocket Engines, Cham,Switzerland: Springer International Publishing, 2021, p. 755.

[7] J. J. Pocha, An Introduction to Mission Design for Geostationary Satellites, 1st Hrsg., Dordrecht: Springer Netherlands, 1987, p. 237.

[8] D. Harrje, LIQUID PROPELLANT ROCKET . COMBUSTION INSTABILITY, Washington, D.C: National Aeronautics And Space Administration, 1972, p. 657.

[9] E. A. Hurlbert, M. J. Atwell, J. C. Melcher und R. L. Morehead, „Integrated Pressure-Fed Liquid Oxygen / Methane Propulsion Systems - Morpheus Experience, MARE, and Future Applications,“ in *52nd AIAA/SAE/ASEE Joint Propulsion Conference.*, Salt Lake City, Utah, USA., 2016-07-25.

[10] J. L. Cannon, „Liquid Propulsion: Propellant Feed System Design,“ in *Encyclopedia of Aerospace Engineering*, L. R. Blockley und W. Shyy, Hrsg., Chichester, UK, Wiley, 2010-12-15, p. 34.